
CIV102 – Structures and Materials

An Introduction to Engineering Design

Part 2: Analysis and Design of Truss Bridges

University of Toronto
Division of Engineering Science
September 2020

Allan Kuan
Michael P. Collins

COPYRIGHT

These course notes are for the exclusive use of students of CIV102 Structures and Materials, an Introduction to Engineering Design at the University of Toronto.



The Quebec Bridge, which opened in 1919, 12 years after the collapse of Theodore Cooper’s original design. Despite opening over 100 years ago, it is still the largest cantilever bridge in the world.

CIV102 Course Notes – Part 2: Analysis and Design of Truss Bridges

Lecture 12 – A Bridge Over Troubled Waters..... 44

Lecture 13 – Truss Analysis: Method of Joints, Method of Sections 48

Lecture 14 – Euler Buckling of Struts 54

Lecture 15 – Truss Bridge Design Continued..... 59

Lecture 16 – Blowing in the Wind..... 64

Lecture 17 – A Bracing Lecture 68

Lecture 18 – Method of Virtual Work 72

Lecture 19 – Where Have All the Soldiers Gone?..... 79

Lecture 12 – A Bridge Over Troubled Waters

Overview:

In this chapter, truss bridge systems are discussed. Trusses, which are assemblies of steel or timber members connected to form lattice-like structures, resist loads by having their members carry axial tension and axial compression forces. The design process for truss bridges is introduced.

Truss Bridges and their Historical Development

Truss bridges were originally used by the Romans, who built them by connecting wooden members to cross distances which were not possible to span using bridges built using post-and-beam construction. None of these early bridges survived after the downfall of the empire, which led to the loss of this style of bridge construction. During the Renaissance era, the Italian architect Andrea Palladio became the first to revive the use of wooden truss bridges and documented his designs in his *Four Books of Architecture*, which were published in 1570. An example of one of his designs, the Bridge of Cismone, is shown below in Fig. 12.2, and described in the excerpt shown in Fig. 12.3.

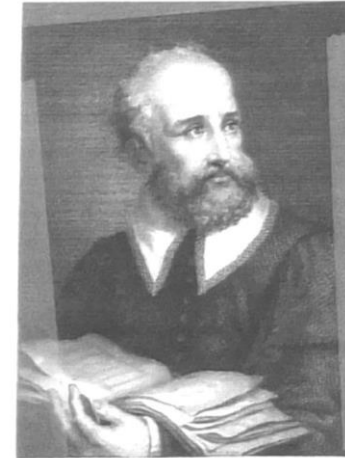


Fig. 12.1 – Portrait of Andrea Palladio, the Italian architect who produced the first written documentation of wooden truss bridges.

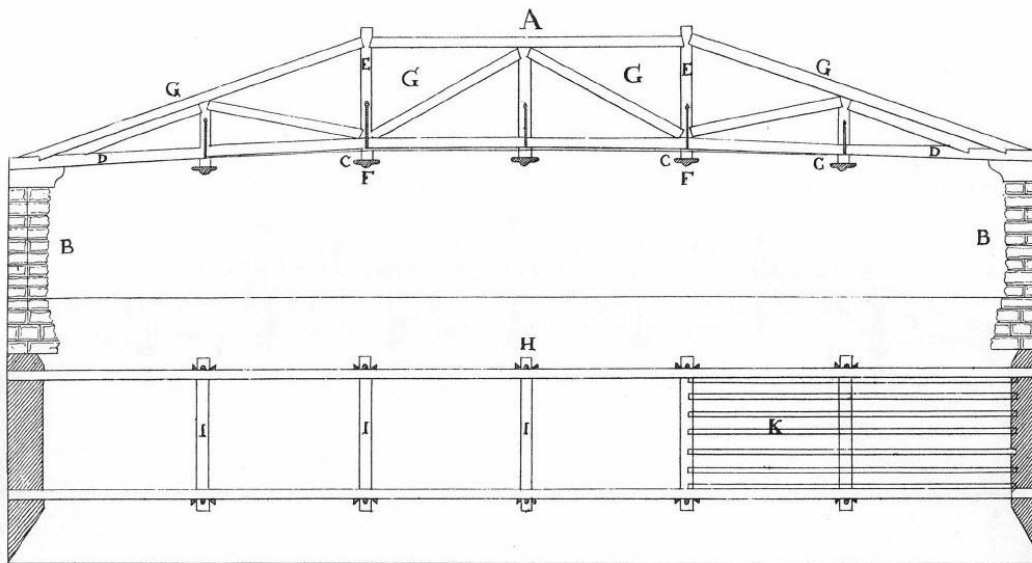


Fig. 12.2 – Elevation (top) and plan (bottom) views of Palladio's Cismone truss bridge

Palladio built his truss bridges by connecting wooden pieces together with iron clamps. Wooden truss bridges based on Palladio's original designs continued to be in use until the early 20th century, when variants built out of cast iron or steel members bolted or riveted together became more common. Modern truss bridges are commonly built using steel members, often hollow tubes, which are bolted or welded together, and are primarily used for pedestrian or railway traffic.

Trusses are an economical structural system for crossing moderate spans because of their efficient use of materials and the fact that they can be analyzed by a design engineer with relative ease. A fundamental assumption is that the connections between the members are rotationally flexible, which allows them to be modelled as pin connections. A consequence of this assumption is that all of the members in the truss will either be in pure tension or pure compression.

Design Process

The process of designing a truss bridge is a straightforward but iterative task. At a high level, the design begins by first determining a suitable arrangement of the members used to cross the span. An estimate of the loads applied to the bridge is then made, and these loads are used to calculate the forces which each member must safely carry. The members are then sized to carry these loads with an appropriate factor of safety. The bridge must then be checked to ensure that it is adequately stiff under service loads and can resist dynamic effects caused by vibrating or moving loads. Finally, the initial estimates of the loads must be verified to ensure that they do not underestimate the actual demand, and then the cost of the structure should be estimated to determine the feasibility of the project. Iteration is often needed to resolve issues which may be encountered during any stage of the design process.

The aforementioned process is explained in more detail below:

1. Define the truss geometry. During this stage of the design process, the span, height, deck width, and configuration of the members must be determined. Increasing the height of the truss at the midspan has the advantage of reducing the magnitude of the forces in the **top** and **bottom chords**, but the increased amount of material needed may make this option uneconomical. Two examples of possible truss geometries are shown in Fig. 12.4 below.

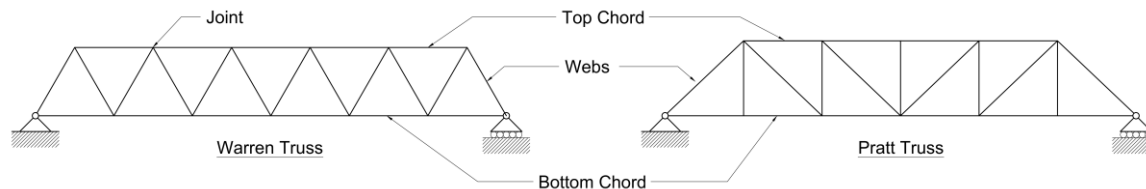


Fig. 12.4 – Examples of common truss designs: Warren truss (left) and Pratt truss (right)

2. Estimate the joint loads. Once the geometry has been determined, the loads which the truss will carry must be obtained. Calculating these loads, which are represented as point loads applied to the truss where the deck meets the structure, is broken down into two processes: (a) estimating the weight carried by the deck due to dead and live loads, which are typically expressed as area loads, and (b) converting these area loads into discrete loads applied to the joints.

The area load applied to the deck due to gravity, w_{total} , is the sum of the deck weight, w_{deck} , the weight of the structural members, w_{struct} , and the live load of a large crowd of people, w_{live} :

$$w_{total} = w_{deck} + w_{struct} + w_{live} \quad (12.1)$$

Note: Efficiency refers to the high strength and stiffness of truss structures relative to its cost and volume of material required to build them.

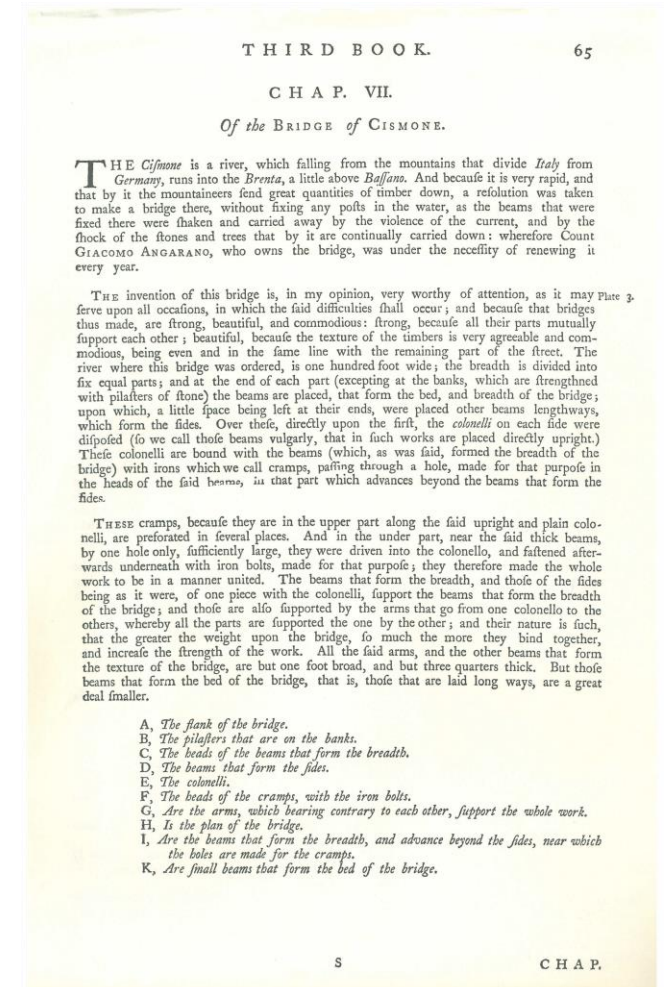


Fig. 12.3 – An excerpt from Palladio's work "I quattro libri dell'architettura" (Four Books of Architecture), describing the design of a wooden truss bridge

When calculating w_{total} , the live load, w_{live} , should be taken as 5.0 kPa, which is approximately equal to 100 lbs/ft². A reasonable estimate of the deck load, w_{deck} , if it is made out of wood is 1.0 kPa, and the weight of the structural members is typically between $w_{struct} = 0.5\text{--}1.0$ kPa when using hollow steel members to span distances of up to 100 m.

Note: The values listed in this paragraph are just suggestions. The actual loads are typically provided by a building standard, or regulatory body, or by a product supplier.

The loads applied to each of the joints, P_i , are obtained by multiplying the area load, w_{total} , by the **tributary area** of the deck, A_{trib} , which is the portion of the deck that the joint is responsible for supporting. This is shown below in Eq. (12.2):

$$P_i = w_{total} A_{trib} \quad (12.2)$$

The tributary area is obtained using the heuristic that each joint is responsible for carrying a deck area which extends halfway towards each of its neighbours. This can be seen in Fig. 12.5, which shows the view of the deck from above:

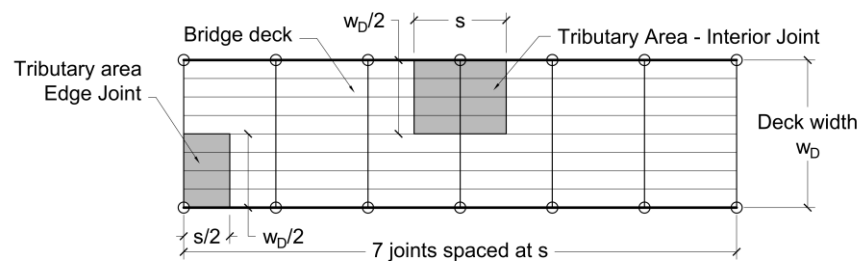


Fig. 12.5 – Plan view of the deck, showing the tributary areas for an interior (middle) and edge (bottom right) joint.

3. Solve for the reaction forces and analyze all of the forces in the members. This step is done using the tools described in Lecture 11 for obtaining the reaction forces, and the analysis methods discussed in Lecture 13.

4. Size the members so that they can safely resist the loads. The method used to proportion the members to resist tension and compression loads is discussed in Lecture 15.

5. Repeat steps 1-4 to design bracing to provide resistance against wind loads and instability effects. In addition to the vertical loads caused by gravity, structures must also resist horizontal loads due to high winds. The cross bracing used to resist the wind loads must also provide adequate support for long members in compression to avoid instability due to buckling. The process of designing braces to fulfill these functions is discussed in Lectures 16 and 17.

6. Calculate the stiffness of the bridge by estimating its deflection at the midspan. A structure must be able to safely carry the applied loads while minimizing the accompanying deformations. A procedure to calculate the deflection of a truss structure called the *Method of Virtual Work* and is described in Lecture 18.

7. Design against dynamic loads. In addition to being able to support a very large, slowly moving crowd of people, a truss bridge must be able to carry a smaller crowd of people walking over the bridge at a brisk pace. In this second situation, the bridge will be subjected to significant dynamic loading which can lead to large displacements and forces due to *resonance*. Lecture 19 presents a simple method for accounting for these dynamic effects.

8. Check if the initial estimate of w_{struct} is greater than the actual weight of the bridge. At the beginning of the design process, an estimate of w_{struct} was needed to proceed with the design. During this stage of the design process, the true weight of the structural components is compared with the initial estimate, and if the initial estimate of w_{struct} is lower than the actual weight, then the design process must be repeated. This requirement is mathematically represented as:

$$w_{struct,actual} = \frac{\sum_{i=1}^n l_i w_i}{L \times w_{deck}} \leq w_{struct,estimate} \quad (12.3)$$

In Eq. (12.3), n is the total number of members in the bridge, l_i and w_i are the length and weight per unit length of each member, L is the span of the bridge and w_{deck} is the width of the deck.

If Eq. (12.3) is not satisfied, the design must begin again from step 2 using a more conservative estimate of w_{struct} .

Lecture 13 – Truss Analysis: Method of Joints, Method of Sections

Overview:

In this chapter, two methods used for the analysis of forces in truss bridges are discussed. The Method of Joints, which uses the two translational equations of equilibrium, is best suited for performing a complete analysis of the forces in a truss structure. On the other hand, the Method of Sections uses all three equations of equilibrium and is a useful technique for checking the forces in the structure at a particular location of interest.

Pre-Analysis Steps

Each of the methods presented herein are used to calculate the forces in the members due to external loads applied to the joints. Joint forces, which are point loads applied to the structure at the joints, can be determined from distributed area loads by using the tributary area concept discussed in Lecture 12. This process is illustrated in Fig. 13.2

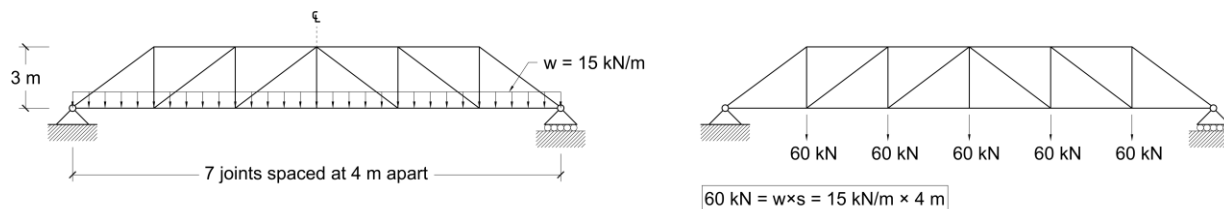


Fig. 13.2 – Truss bridge with distributed loads (left) and equivalent joint loads (right)

Once the joint loads have been determined, the reaction forces can be calculated using the three equations of equilibrium. For a simply supported structure supported by a pin and roller on its two ends and carrying a uniform pedestrian load, the vertical reactions are equal to half of the total load due to symmetry. More complicated cases involving non-symmetric load patterns require using the full set of equilibrium equations to get the reaction forces.

Fig. 13.3 shows a truss structure whose loads have been converted to joint loads and has had its reaction forces determined. The structure is now ready to have its member forces determined using either the Method of Joints or Method of Sections.

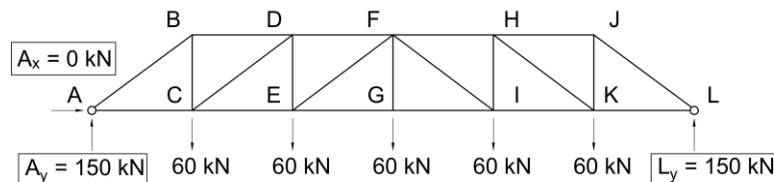


Fig. 13.3 – Truss structure with joint loads and solved reaction forces

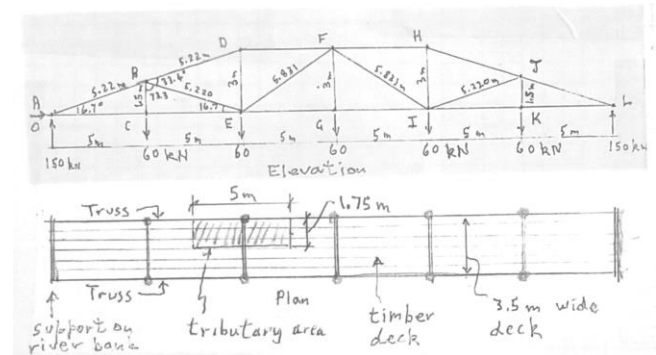


Fig. 13.1 – Summary of truss analysis for Palladio's truss bridge over the Cismone River

Method of Joints

Conceptually, the Method of Joints involves evaluating the state of equilibrium in the structure one joint at a time. At each joint, the two translational equations of equilibrium are used to solve for the unknown forces carried in the members framing into the joint. Finding all of the forces in the structure is done joint-by-joint, two forces at a time.

To illustrate how the Method of Joints works, we will apply it to the truss structure shown in Fig. 13.3 which has 12 joints and 21 member forces. Due to symmetry, the number of unknown member forces can be reduced to 11, which is solvable by examining 6 joints. We will begin the analysis at joint A which has only two unknown member forces; with the exception of joint L, the other joints cannot be used as a starting point because they each contain three or more unknown member forces, which is greater than the two equations of equilibrium we have at our disposal.

When drawing a free body diagram at a joint, both the external forces applied to the joint (due to the reaction loads or applied loads) and the internal forces in the attached members must be considered. To illustrate this, Fig. 13.4 shows a free body diagram of joint A, showing two unknown member forces, AB and AC, as well as the reaction forces, A_x and A_y (note that $A_x = 0$).

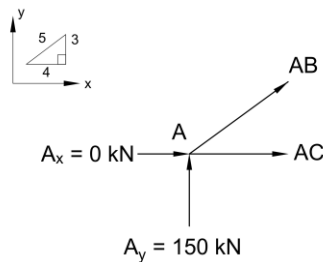


Fig. 13.4 – Free Body Diagram of joint A

The corresponding equations of equilibrium are:

$$\sum F_x = 0 \rightarrow A_x + AB_x + AC_x = 0 \quad (13.1)$$

$$\sum F_y = 0 \rightarrow A_y + AB_y = 0 \quad (13.2)$$

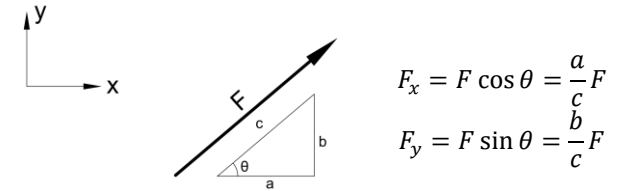
Substituting $A_y = 150$ kN into Eq. (13.2) and solving for AB results in the following:

$$AB_y = -150 \rightarrow AB = \frac{5}{3} \times (-150) = -250 \text{ kN} \quad (13.3)$$

Once the force in member AB is known, the force in member AC can be determined using Eq. (13.1):

$$AC = AC_x = -AB_x \rightarrow AC = -\frac{4}{5} \times (-250) = +200 \text{ kN} \quad (13.4)$$

Note: Recall that for a member carrying an axial force F , its x - and y - components F_x and F_y are related to F by the inclination of the member:



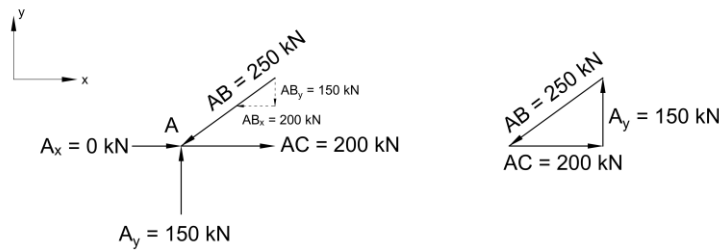


Fig. 13.5 – Summary of member forces framing into joint A

After solving for the unknown forces, it is helpful to summarize them in a diagram like the one shown in the left free body diagram in Fig. 13.5. Because we found that the force in member AB was a negative number using our initial sign convention in Fig. 13.4, the direction has been reversed in Fig. 13.5. The x- and y- components of AB are also shown, which allows the state of equilibrium at joint A to be easily checked. Furthermore, it is clear that member AB is in compression as it pushes into joint A, and member AC is in tension as it pulls away from joint A.

The force vector diagram in Fig. 13.5 graphically illustrates equilibrium of the joint by rearranging the forces in the free body diagram so that the tails and tips of each force are connected. Equilibrium is satisfied because the rearranged force vectors are able to form a closed path.

Once the forces in member AB and AC have been solved by analyzing joint A, the process is repeated at an adjacent joint to solve for more unknown member forces. Joints B and C are possible candidates; however, joint C has three unknown member forces and hence cannot be solved yet. Therefore, we will move to joint B which only has two unknown forces to solve.

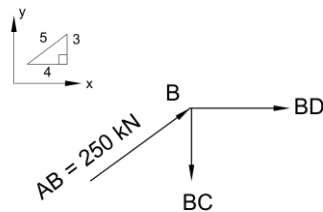


Fig. 13.6 – Free Body Diagram of joint B

A free body diagram of joint B is shown in Fig. 13.6, which contains two unknown member forces, BC and BD, and force AB which we solved at joint A. Note the sign convention used to define the direction of the three forces: BC and BD are assumed to be in tension and pull away from the joint. AB, which was determined to be in compression from our analysis of joint A, is directed to push into joint B with a magnitude of 250 kN. The resulting equations of equilibrium are the following:

Note: It is very easy to make errors with the sign convention and accidentally identify tension members as compression members and vice versa. Note the following rules:

- If a force is assumed to pull away from the joint but is calculated to be negative using the corresponding equilibrium equations, then the member is in compression.
- If a force is assumed to push into a joint but is calculated to be negative using the corresponding equilibrium equations, then the member is in tension.

Extra care must be taken when carrying over the results from one joint to solve for the forces in an adjacent joint.

Note: Although it is not immediately obvious how to determine if a member is in tension or compression based on a free body diagram of a joint, it is helpful to think of Newton's third law:

- If a member is in tension, the joints apply forces to the members which pull away from the member. To resist these forces, the member applies forces to the joints which pulls them together.
- If a member is in compression, the joints apply forces to the member which push into the member. To resist these forces the member applies forces to the joints to push them apart.

These principles are illustrated in Fig. 13.7 below:

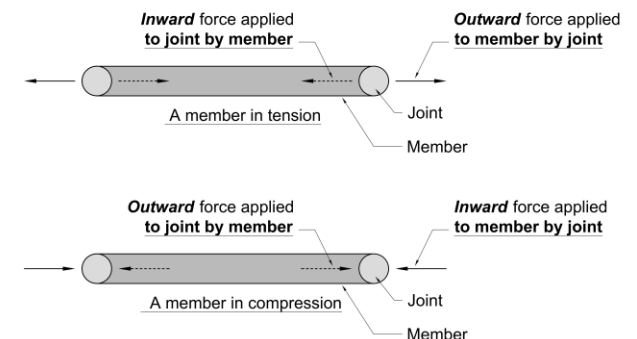


Fig. 13.7 – Compression and tension forces

$$\sum F_x = 0 \rightarrow AB_x + BD = 0 \quad (13.5)$$

$$\sum F_y = 0 \rightarrow AB_y - BC = 0 \quad (13.6)$$

Solving for BC and BD can then be done by substituting the magnitude of the compression force in AC, 250 kN, into Eq. (13.5) and (13.6), which results in:

$$BD = -AB_x = -\frac{4}{5} \times (250) = -200 \text{ kN} \quad (13.7)$$

$$BC = AB_y = \frac{3}{5} \times (250) = +150 \text{ kN} \quad (13.8)$$

Summarizing these forces into the free body diagram shown below in Fig. 13.8 shows that member BD, like member AB, is in compression as it applies a force which pushes into joint B. Member BC on the other hand is in tension, applying a force which pulls away from joint B. The force vector diagram also shown in Fig. 13.8 also demonstrates that the joint is in equilibrium.

Note: When interpreting a free body diagram of the joint, remember that the forces drawn in are the forces applied by the member to the joint.

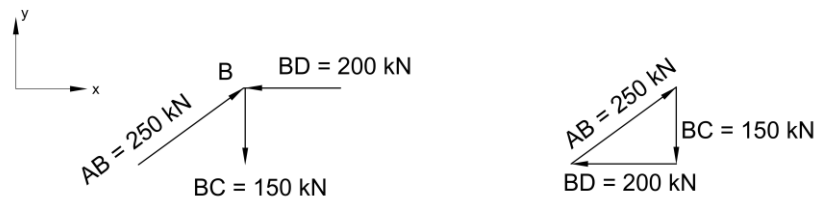


Fig. 13.8 – Summary of member forces framing into joint B

With these results, the process continues at joint C, and repeats until all of the member forces have been found. The results of the complete analysis are shown below in Fig. 13.9, with tension forces indicated as positive and compression forces indicated as negative.

Note: When presenting your solutions on assignments, quizzes and on the final exam, follow the same sign convention: members in tension are positive, and members in compression are negative.

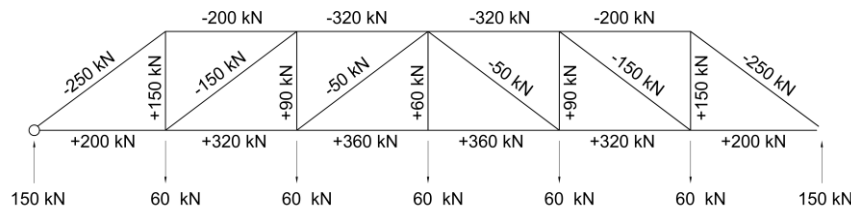


Fig. 13.9 – Summary diagram showing the solved member forces in the truss bridge

Method of Sections

Although the Method of Joints is a robust tool for solving for all of the forces in a truss structure, solving for member forces which are located far away from the starting point, like the ones close to the midspan in Fig. 13.9, is a tedious process because they can only be found after the forces closer to the supports are known. A faster method to solve for these forces, which is suitable for checking the correctness of the results or performing a preliminary design, is to instead use the Method of Sections.

The Method of Sections uses the three equations of equilibrium to solve for up to three unknown member forces which pass through a “section” of the truss structure. Using the method first involves cutting the structure apart with a line passing through the three members of interest. The equations of equilibrium are then applied to either of the resulting two substructures to solve for the unknown internal forces which were revealed by the section cut.

To illustrate how to apply the Method of Sections, we will solve for the forces in members DF, EF and EG from our previous example. Figure 13.10 shows two free body diagrams, one for the left substructure and one for the right substructure, after the original structure was cut through these members. Because the original structure was in equilibrium, each substructure must also be in equilibrium and hence the forces of interest can be determined by examining either of the free body diagrams.

Note: Defining the initial directions of the unknown forces is very important when using the Method of Sections. If the unknown forces are assumed to pull away from the joints, then positive values will correspond to tension and negative values will correspond to compression.

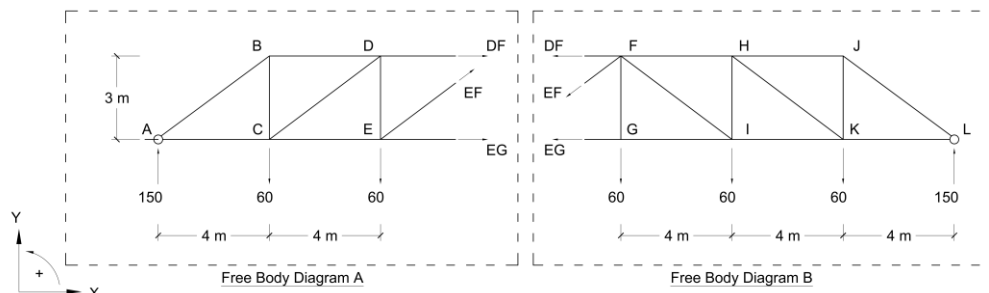


Fig. 13.10 – Free body diagrams used in the Method of Sections to solve DF, EF and EG

In Free Body Diagram A, the translational equilibrium equations can be written as:

$$\sum F_x = 0 \rightarrow DF + EF_x + EG = 0 \quad (13.9)$$

$$\sum F_y = 0 \rightarrow 150 + EF_y - 60 - 60 = 0 \quad (13.10)$$

When considering rotational equilibrium, the number of unknown forces which appears in the equation depends on the choice of reference point. A good choice of reference point in this example is joint E, which has two unknown forces, EF and EG passing through it, meaning that the resulting equation will only contain one unknown force, DF. In general, it is a good idea to select a point which is common to two of the forces which need to be solved. The resulting equation is shown below:

Note: The resulting equations of equilibrium should only include the reaction force at a support, the joint loads applied to the substructure, and the three unknown internal forces which were revealed by the cut.

$$\sum M_E = 0 \rightarrow 60 \times 4 - 150 \times 8 - DF \times 3 = 0 \quad (13.11)$$

Eqs. (13.9) to (13.11) are a system of three equations with three unknowns (DF, EF, and EG), which when solved results in $DF = -320$ kN, $EF = -50$ kN and $EG = +360$ kN. These results are consistent with our full solution shown in Fig. 13.9.

Note that examining equilibrium of Free Body Diagram B in Fig. 13.10 would result in the same values of DF, EF and EG.

Lecture 14 – Euler Buckling of Struts

Overview:

Slender members in compression can fail suddenly due to buckling. This chapter presents the derivation of Euler's equation for predicting the load at which buckling takes place.

Members in Compression

Consider the prismatic member shown in Fig. 14.2. If the two ends of the member are subjected to tensile forces T , the only way for the ends of the member to move apart is if the member elongates. The strains experienced by the member as it stretches can be calculated using the equation $\varepsilon = \Delta l / L_0$, and the member will fail when the stress in the member, $\sigma = T/A$, is equal to the ultimate tensile strength of the material.

Consider the members subjected to compression forces in Fig. 14.3. Under the compressive forces, the two ends of the member are forced to come together. However, unlike the member in tension, there are two possible ways for the member to deform to allow these points to come together. The first way is for the member to simply shorten, which is the opposite of what would happen if it was instead in tension. The second way is if the member, instead of changing length, curves to bring the two ends together. These two actions are shown on the central and right figures in Fig. 14.3 respectively.

Failure due to the first mode of deformation, which typically occurs for short, stocky members, is called **crushing**, and the force which causes crushing is sometimes referred to as the **squash load**. The second mode of failure, which commonly occurs in long, slender members, is called **buckling**. How a member fails depends on the relative amount of force required to cause crushing or buckling; whichever is easier will be the cause of failure.



Fig. 14.1 – Soviet-era stamp celebrating the 250th birthday of the famous mathematician Leonard Euler.

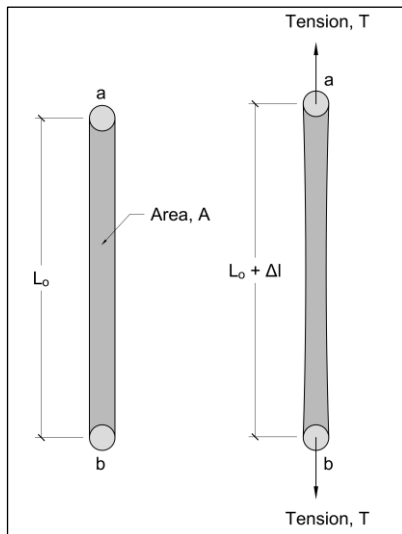


Fig. 14.2 – Members in tension

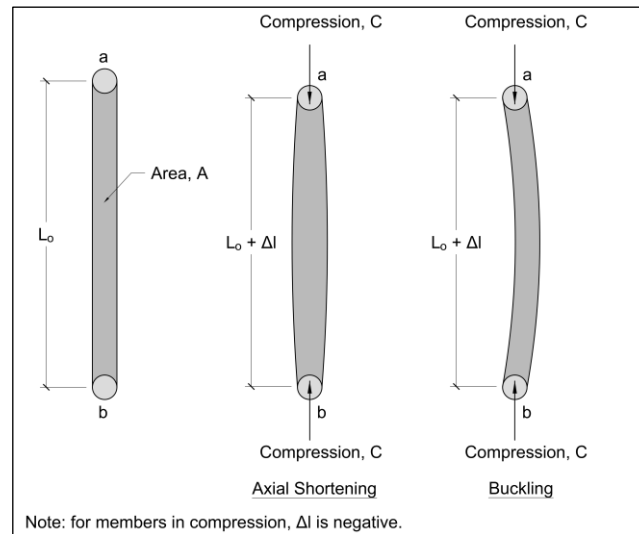


Fig. 14.3 – Members in compression

Calculating the squash load of a member, P_{crush} , is straightforward if the cross-sectional area A and the ultimate compressive stress, σ_{crush} , are known:

$$P_{\text{crush}} = \sigma_{\text{crush}} A \quad (14.1)$$

Calculating the load which causes buckling to take place is more challenging because failure involves the member bending. The solution to the buckling problem was eventually solved by Leonhard Euler in 1757, leading to his celebrated equation for the Euler load, or the load causing buckling, P_e :

$$P_e = \frac{\pi^2 EI}{L^2} \quad (14.2)$$

Derivation of the Euler Load for Elastic Buckling

Euler's derivation of the buckling equation begins with the following assumptions on the member, shown in Fig. 14.4, which has a length of L and is being subjected to a compression force P which causes the member to curve as it buckles:

- The material is homogenous and linear elastic, having a uniform Young's modulus, E , and second moment of area, I .
- The top and bottom ends of the member are free to rotate. Furthermore, the top of the member is free to move vertically and the bottom of the member is translationally fixed in place.
- The member is initially perfectly straight and either end is free to translate horizontally.

Note: Recall that the product EI is the flexural stiffness of a member.

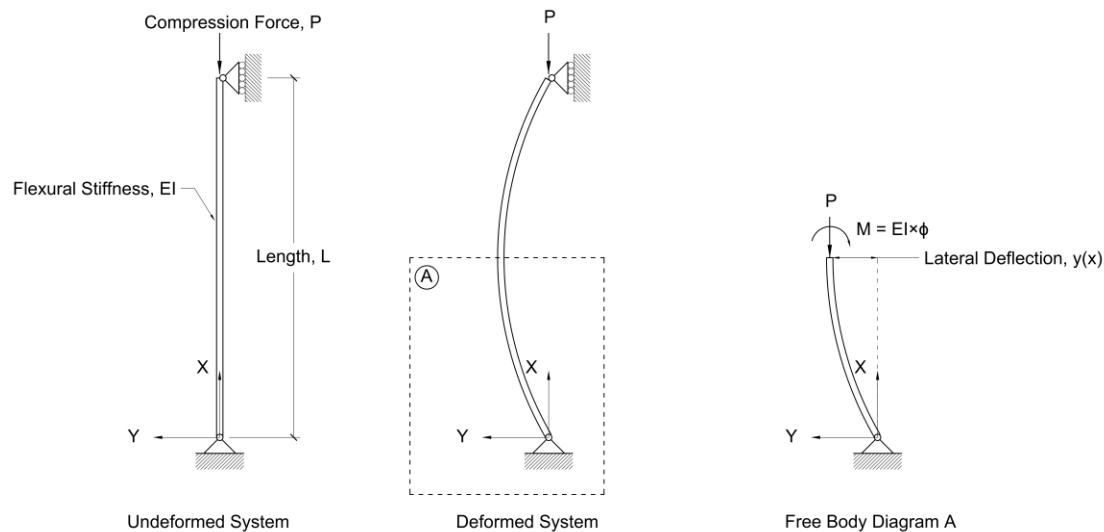


Fig. 14.4 – Derivation of Euler's critical buckling load

To investigate how the member is resisting the load while in its curved position, a free body diagram can be drawn which cuts through the member a distance x away from the pin support. At the cut, the member is transmitting the compressive force \mathbf{P} , which forms a counterclockwise couple with the reaction force at the base. To resist this couple, the bent member must also carry a moment \mathbf{M} at the location of the cut, which rotates clockwise to satisfy rotational equilibrium. Taking the sum of moments to equal to zero results in the following equation:

$$P \times y = M \quad (14.3)$$

In Eq. (14.3), y is the lateral displacement of the member relative to its original position. Recall that the moment carried by the member is related to its curvature, ϕ , by the flexural stiffness \mathbf{EI} :

$$M = EI\phi \quad (14.4)$$

Substituting Eq. (14.4) into Eq. (14.3) the results in the following equation:

$$Py = EI\phi \quad (14.5)$$

Recall that the curvature is defined as the change in slope along the length of the member, and the slope is the change in lateral displacement. Therefore, the curvature is the second derivative of the lateral displacement; noting that the member has displaced in the positive y direction but is concave down, ϕ and y have the following relationship:

$$\phi = -\frac{d^2y}{dx^2} \quad (14.6)$$

Substituting Eq. (14.6) into Eq. (14.5) and then dividing both sides by \mathbf{EI} results in the following differential equation:

$$\frac{P}{EI}y = -\frac{d^2y}{dx^2} \quad (14.7)$$

We can solve Eq. (14.7) in the same way that we solved the differential equation for free vibrations in Lecture 7, which was by assuming a function for y , and then checking to see that it satisfies the equation. Because Eq. (14.7) resembles the differential equation that we saw in Lecture 7, we will assume that y has the form:

$$y = A \sin(\omega x + B) \quad (14.8)$$

Taking the second derivative of Eq. (14.8) and then substituting everything into Eq. (14.7) results in the following requirement for ω :

$$\omega = \sqrt{\frac{P}{EI}} \quad (14.9)$$

We can learn more about the shape of the buckled member if we make use of the fact that the member is prevented from having any lateral displacements at its ends. These are summarized in the following **boundary conditions**:

$$y(x = 0) = 0; y(x = L) = 0 \quad (14.10)$$

Substituting the first boundary condition into Eq. (14.8) results in the requirement that $\mathbf{B} = 0$:

$$0 = A \sin(\omega \times 0 + B) \rightarrow B = 0 \quad (14.11)$$

Using this new information and then substituting the second boundary equation into Eq. (14.8) results in the requirement that ωL be an integer multiple of π (i.e. $\mathbf{n} = 0, 1, 2, 3$, etc.):

$$0 = A \sin(\omega L) \rightarrow \omega L = n\pi \quad (14.12)$$

Combining Eq. (14.9) with Eq. (14.12) and isolating for the load carried by the buckled member, \mathbf{P} , results in the following equation:

$$P = \frac{n^2 \pi^2 EI}{L^2} \quad (14.13)$$

The smallest nonzero value of \mathbf{P} requires using $n = 1$. This corresponds to the Euler load in Eq. (14.2), which is reproduced below as Eq. (14.14):

$$P_e = \frac{\pi^2 EI}{L^2} \quad (14.14)$$

Higher Modes of Buckling

Note that in our equation for \mathbf{P} , the compressive force carried by the buckled member, there were numerous values of \mathbf{n} which were possible. Values of \mathbf{n} which are higher than $n = 1$ correspond to higher modes of buckling, which occur when the member buckles into more complex shapes. For the simple member used in this example, \mathbf{n} corresponds to the number of half cycles that the sinusoidally-shaped member assumes. The shapes corresponding to various values of \mathbf{n} are shown in Fig. 14.5.

Stability of Members under Compression Loads

Buckling is an unstable form of equilibrium. Unlike tension for example, where pulling on a member produces a restoring force which helps to return the member back to its original shape, a member which is buckling will continuously weaken and curve more and more as it is loaded.

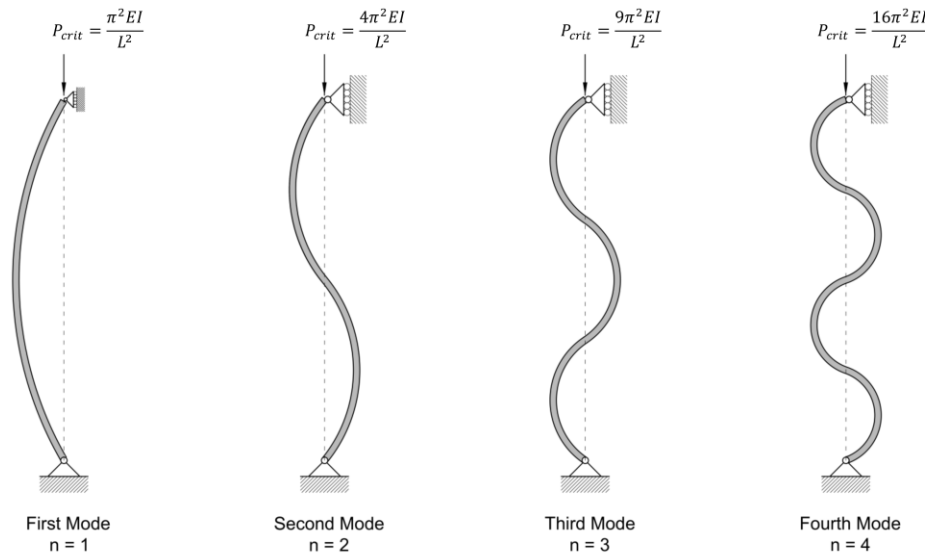


Fig. 14.5 – Higher modes of buckling and associated critical buckling loads

Under ideal conditions, members are perfectly straight and will theoretically remain so before suddenly buckling once the critical buckling load is reached. Real members however are not perfect and will have a nonzero initial lateral deflection at their midspan, Δ_o because they are not straight. This initial deflection means that they will visibly bend before the Euler load is reached. The relationship posed by the British mathematician Richard Southwell suggests that that lateral deflection of an imperfect member, Δ_{lat} , when subjected to a compression force P is:

$$\Delta_{lat} = \frac{\Delta_o}{1 - \frac{P}{P_{crit}}} \quad (14.15)$$

In Eq. (14.15), P_{crit} is the critical buckling load, which is equal to the Euler load for members which satisfy the support conditions used to derive P_e . The behaviour predicted by Eq. (14.15) is compared with ideal buckling behaviour in Fig. 14.6.

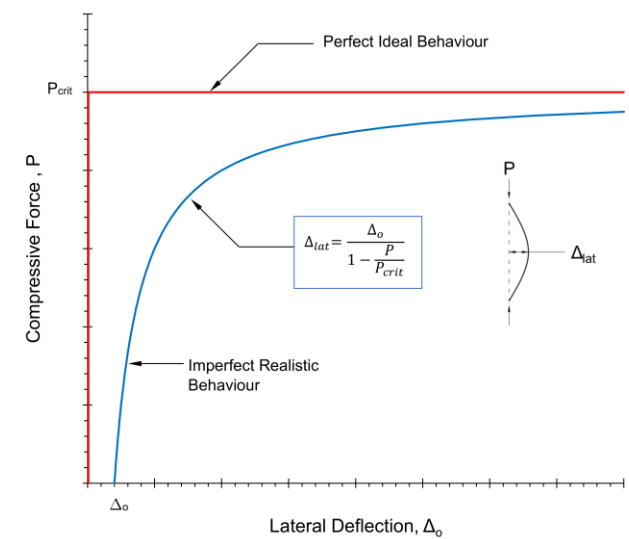


Fig. 14.6 – Comparison of compression response for perfect (red) and imperfect (blue) members

*Note: The response of ideal members which remain perfectly straight before buckling at the Euler load is an example of **bifurcation behaviour**.*

Note: A graphical representation of Southwell's method can be used to determine the critical buckling load of an as-built member without subjecting it to forces which approach its failure load. This is useful for evaluating the safety of structures which are in service and cannot be loaded to failure.

Lecture 15 – Truss Bridge Design Continued

Overview:

In this chapter, the process for selecting appropriate members in a steel truss using working stress design is discussed. The properties of hollow structural sections (HSS) are described in detail. Although the design of truss members using steel HSS are covered in this chapter, the basic concepts are also applicable to the design of trusses using other materials (i.e. wood) or alternative types of steel sections.

Design of Members in Tension

As discussed in Lecture 6, steel behaves in a linear elastic manner for relatively small stresses. Once the stress in the material reaches the yield stress, it will yield and elongate substantially, with most of these deformations being non-recoverable. The steel will be able to resist a higher stress than the yield stress, the ultimate stress, due to the effects of strain hardening, before failing shortly after.

Although designing structures using the ultimate strength can lead to material savings, structures must prioritize safety over economy. This is because the consequences of exceeding the ultimate stress, which include structural failure and a potentially catastrophic loss of life, are not worth the relatively minor savings in the cost of construction. It is for this reason that the yield strength is instead used as the design strength of the materials involved. Furthermore, large factors of safety are employed to further reduce the potential of failure, as discussed in Lecture 8, and guarantee that the structure remains in a linear elastic state during its service life.

Note: Another reason why the yield strength is used instead of the ultimate strength is because the significant permanent deformations due to yielding are not desirable. Although structures which have yielded may still be strong enough to carry substantial forces, they will appear undesirable and may not be able to fulfill their other non-structural functions.

The stress, σ , in a member with a cross sectional area A when it is carrying a tension force F is:

$$\sigma = \frac{F}{A} \quad (15.1)$$

In design, the maximum allowable stress which may be carried by a member in tension is the yield stress, σ_y , divided by a factor of safety; an appropriate factor of safety for yielding is $FOS_{yield} = 2.0$. Substituting this into Eq. (15.1) results in the following requirement on the cross-sectional area of a member which must carry a tensile force F :

$$A \geq FOS_{yield} \frac{F}{\sigma_y} = 2.0 \frac{F}{\sigma_y} \quad (15.2)$$

A common value of the yield strength of structural steel products made in Canada is $\sigma_y = 350 \text{ MPa}$.

Design of Members in Compression

Members in compression can fail by either crushing or by buckling. Crushing failures, which occur in stocky members which do not buckle, occur when the stresses reaches the compressive strength of the material. For steel, the stress which causes yielding in compression is the same as the yield stress in tension, which is 350 MPa. Therefore, Eq. (15.2), using a factor of safety of 2.0 for yielding in compression, can also be used to determine the required cross-sectional area for members in compression.

Buckling occurs when the load carried by the member reaches its critical buckling load, P_e . Recall that for a member with Young's Modulus E , second moment of area I and length L , the buckling load is equal to:

$$P_e = \frac{\pi^2 EI}{L^2} \quad (15.3)$$

Buckling is a more dangerous mode of failure than yielding. Some reasons why this is the case are because it generally occurs more suddenly and is associated with instability and a loss of strength in the member once it takes place. Therefore, the factor of safety associated with buckling is $FOS_{buckling} = 3.0$, which is larger than the corresponding factor of safety for the above reasons. Reducing the allowable compressive force by taking P_e and dividing it by the factor of safety results in the following requirement on the second moment area of a member which must carry a compression force F :

$$I \geq FOS_{buckling} \frac{FL^2}{\pi^2 E} = 3.0 \frac{FL^2}{\pi^2 E} \quad (15.4)$$

As noted in earlier chapters, the Young's modulus of steel is $E = 200,000 \text{ MPa}$.

The stress causing failure of a member subjected to compression forces is the smaller of the failure stresses associated with yielding and buckling. The yield stress is a property of the material and is independent of its size. On the other hand, the Euler buckling stress σ_e which is calculated by taking the buckling load P_e and dividing by the cross-sectional area A , depends on the length of the member, L :

$$\sigma_e = \frac{P_e}{A} = \frac{\pi^2 EI}{AL^2} \quad (15.5)$$

We can simplify Eq. (15.5) by introducing a new term r , which is called the **radius of gyration**:

$$r = \sqrt{\frac{I}{A}} \quad (15.6)$$

Substituting the definition of r into Eq. (15.5) results in the following representation of the buckling stress:

$$\sigma_e = \frac{\pi^2 E}{(L/r)^2} \quad (15.7)$$

In Eq. (15.7), L/r is called the **slenderness ratio**, and is a nondimensional term which describes the tendency of a member to buckle. Members with a large slenderness ratio tend to fail due to buckling, and those with a small slenderness ratio tend to fail by crushing.

Note: The radius of gyration is not a directly measurable property and is not equal to the radius of a circle. Its meaning can be obtained by considering that I is the geometric property of a cross section which affects its flexural stiffness, and A is the geometry property which affects its axial stiffness. The radius of gyration is hence a ratio of a member's flexural stiffness compared to its axial stiffness.

Fig. 15.1 plots the failure stress of members in compression as a function of the slenderness ratio of the member. For short members with low slenderness ratios, the buckling stress approaches infinite and hence these members instead fail at the yield stress of the material. However, as the slenderness ratio increases, the buckling stress decreases rapidly which causes very slender members to fail at a fraction of the yield stress of the material. The red curve, which is obtained by taking the smaller of the yield stress and the buckling stress, represents the failure stress of the member and is often referred to as a **failure envelope**. The blue curve is obtained in a similar manner as the failure envelope but considers the minimum of the allowable yield stress and the allowable buckling stress. This curve is suitable for design because it incorporates appropriate factors of safety for the two modes of failure.

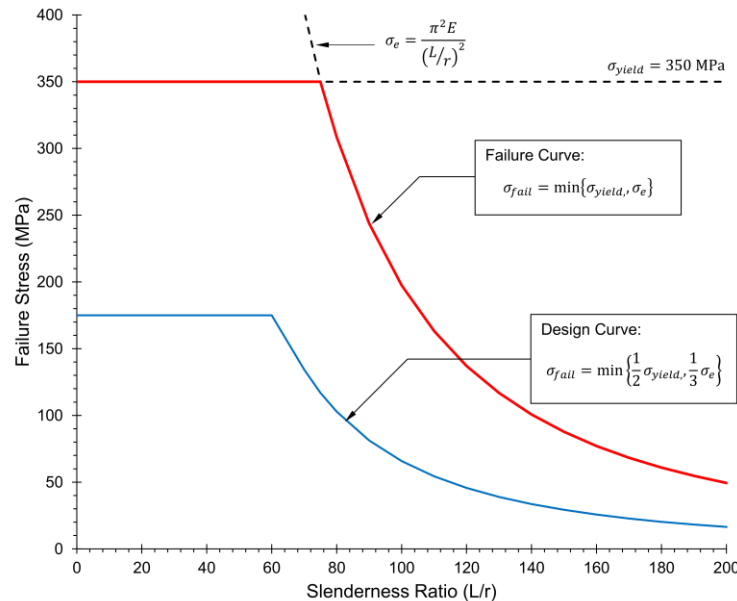


Fig. 15.1 – Influence of slenderness ratio on the strength of compression members. Values plotted are for steel with $\sigma_y = 350 \text{ MPa}$ and $E = 200,000 \text{ MPa}$.

Summary of Design Requirements

When designing the individual members used in a structure, the primary task required of an engineer is to proportion the sizes of the members so that they are able to safely resist the applied loads. Once the minimum required values of cross-sectional properties, such as the cross-sectional area **A**, second moment of area **I**, and radius of gyration **r**, have been obtained, the structural member is specified from a catalogue of available products.

Eq. (15.2) is appropriate for selecting the required **A** for both tension and compression members. The minimum required **I** for compression members can be determined by using Eq. (15.4); this check is not required for tension members which cannot buckle. Furthermore, modern design codes also limit the slenderness ratio of a member to discourage the use of very slender members which are vulnerable to unexpected changes in loading. This requirement is shown in Eq. (15.8):

Table 15.1 – Design Equations for Tension and Compression Members

Member Type	Cross-Sectional Area, A	Second Moment of Area, I	Radius of Gyration, r
Tension Members	$A \geq 2.0 \frac{F}{\sigma_y}$	N/A	$r \geq \frac{L}{200}$
Compression Members		$I \geq 3.0 \frac{FL^2}{\pi^2 E}$	

$$\frac{L}{r} \leq 200 \quad (15.8)$$

A summary of equations used to design tension and members used in truss structures is shown in Table 15.1

Steel Truss Design using Hollow Structural Sections

Steel is a common building material used in civil construction, and a particularly common family of steel members used in steel truss bridges are ***hollow structural sections*** (HSS). HSS are hollow steel tubes which are formed by rolling sheets of steel to form members which are square, rectangular or circular in cross section. Being hollow, HSS members are relatively light, and being made of steel, can be both strong and stiff. HSS are sold by many steel fabricators in commonly produced sizes, some of which are shown in Table 15.2 which is reproduced in Appendix B.

Fig. 15.2 shows the cross sections of a square (left) and rectangular (right) HSS, which have the height, width and thickness as key geometric properties. Many types of HSS which have the same outside dimensions can be ordered in various thicknesses. HSS are typically specified in engineering drawings and specifications using their nominal dimensions. For example, an HSS 305x203x13 is a rectangular HSS which is nominally 305 mm tall, 203 mm wide and has a nominal wall thickness of 13 mm.

Typically, when designing with HSS, it is common to use one continuous member size for the entire bottom chord of a bridge, and one continuous member size for the entire top chord. The web members, which should be smaller than the chords to facilitate the process of connecting the members together, can be individually sized to match the anticipated forces that they must carry. However, it is advisable to only choose one or two members for the webs to reduce the likelihood of errors during construction.

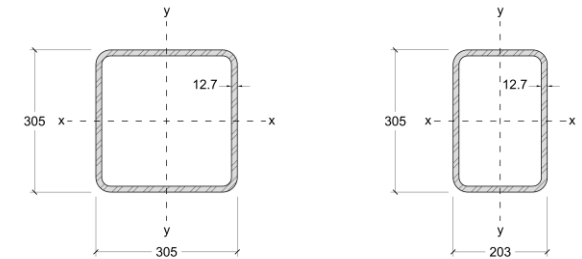


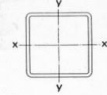
Fig. 15.2 – HSS 305x305x13 (left) and HSS 305x203x13 (right)

*Note that the **designation** of an HSS, which refer to the nominal dimension of the section, is different than the **size** of the HSS, which refer to the actual dimensions. In reality, an HSS 305x203x13 will have a wall thickness of 12.7 mm, not 13 mm.*

Table 15.2 – Table of Standard HSS Properties

STEEL

SQUARE Hollow Structural Sections

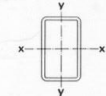


METRIC Dimensions and Properties

Designation	Size	Mass	Dead Load	Area	I	S	r	Z	Torsion J	Surface Area	Shear C _{rt}
mm x mm x mm	mm x mm x mm	kg/m	kN/m	mm ²	10 ⁶ mm ⁴	10 ³ mm ³	mm	10 ³ mm ³	10 ³ mm ³	m ² /m	mm ²
HSS 305x305x13	HSS 305x305x12.7	113	1.110	14 400	202	1 330	118	1 560	324 000	1.18	6 450
x 11	x 11.1	100	0.982	12 800	181	1 190	119	1 380	288 000	1.18	5 790
x 9.5	x 9.53	86.5	0.848	11 000	158	1 040	120	1 210	250 000	1.19	5 080
x 8.0	x 7.95	72.8	0.714	9 280	135	886	121	1 030	211 000	1.19	4 340
x 6.4	x 6.35	58.7	0.576	7 480	110	723	121	833	171 000	1.20	3 550
HSS 254x254x13	HSS 254x254x12.7	93.0	0.912	11 800	113	888	97.6	1 060	183 000	0.972	5 160
x 11	x 11.1	82.4	0.808	10 500	102	799	98.4	945	163 000	0.978	4 660
x 9.5	x 9.53	71.3	0.699	9 090	89.3	703	99.1	825	142 000	0.983	4 110
x 8.0	x 7.95	60.1	0.590	7 660	76.5	602	99.9	720	121 000	0.989	3 530
x 6.4	x 6.35	48.6	0.476	6 190	62.7	494	101	571	97 900	0.994	2 900
HSS 203x203x13	HSS 203x203x12.7	72.7	0.713	9 260	54.7	538	76.8	650	90 700	0.769	3 870
x 11	x 11.1	64.6	0.634	8 230	49.6	488	77.6	584	81 200	0.775	3 530
x 9.5	x 9.53	56.1	0.550	7 150	43.9	432	78.4	513	71 000	0.780	3 150
x 8.0	x 7.95	47.5	0.465	6 050	37.9	373	79.2	438	60 500	0.786	2 730
x 6.4	x 6.35	38.4	0.377	4 900	31.3	308	79.9	359	49 300	0.791	2 260
HSS 178x178x13	HSS 178x178x12.7	62.6	0.614	7 970	35.2	396	66.4	494	59 200	0.688	3 230
x 11	x 11.1	55.7	0.547	7 100	32.1	361	67.2	436	53 200	0.673	2 970
x 9.5	x 9.53	48.5	0.476	6 180	28.6	322	68.0	365	46 700	0.678	2 660
x 8.0	x 7.95	41.1	0.403	5 240	24.8	279	68.8	330	39 900	0.684	2 320
x 6.4	x 6.35	33.4	0.327	4 250	20.6	231	69.6	271	32 700	0.689	1 940
x 4.8	x 4.78	25.5	0.250	3 250	16.1	181	70.3	209	25 200	0.695	1 520
HSS 152x152x13	HSS 152x152x12.7	52.4	0.514	6 680	21.0	275	56.0	341	36 000	0.566	2 580
x 11	x 11.1	46.9	0.460	5 970	19.3	253	56.8	310	32 500	0.571	2 400
x 9.5	x 9.53	40.9	0.401	5 210	17.3	227	57.6	275	28 700	0.577	2 180
x 8.0	x 7.95	34.8	0.341	4 430	15.1	198	58.4	237	24 600	0.582	1 920
x 6.4	x 6.35	28.3	0.278	3 610	12.6	166	59.2	195	20 300	0.588	1 610
x 4.8	x 4.78	21.7	0.213	2 760	9.93	130	59.9	152	15 700	0.593	1 270
HSS 127x127x11	HSS 127x127x11.1	38.0	0.373	4 840	10.4	164	46.4	205	18 000	0.470	1 840
x 9.5	x 9.53	33.3	0.327	4 240	9.47	149	47.2	183	16 000	0.475	1 690
x 8.0	x 7.95	28.4	0.279	3 620	8.35	132	48.0	159	13 900	0.481	1 510
x 6.4	x 6.35	23.2	0.228	2 960	7.05	111	48.8	132	11 500	0.486	1 290
x 4.8	x 4.78	17.9	0.175	2 280	5.60	88.1	49.6	103	8 920	0.492	1 030
HSS 102x102x9.5	HSS 102x102x9.53	25.7	0.252	3 280	4.44	87.4	36.8	110	7 740	0.374	1 210
x 8.0	x 7.95	22.1	0.217	2 820	3.98	78.4	37.6	96.6	6 780	0.379	1 110
x 6.4	x 6.35	18.2	0.178	2 320	3.42	67.3	38.4	81.3	5 670	0.385	968
x 4.8	x 4.78	14.1	0.138	1 790	2.75	54.2	39.2	64.3	4 450	0.390	789
HSS 89x89x9.5	HSS 88.9x88.9x9.53	21.9	0.215	2 790	2.79	62.7	31.6	80.2	4 970	0.353	968
x 8.0	x 7.95	18.9	0.186	2 410	2.53	57.0	32.4	71.2	4 390	0.358	908
x 6.4	x 6.35	15.6	0.153	1 990	2.20	49.5	33.2	60.5	3 700	0.364	806
x 4.8	x 4.78	12.2	0.119	1 550	1.79	40.3	34.0	48.2	2 930	0.369	667
HSS 76x76x8.0	HSS 76.2x76.2x7.95	15.8	0.155	2 010	1.49	39.0	27.2	49.7	2 630	0.278	706
x 6.4	x 6.35	13.1	0.129	1 670	1.31	34.4	28.0	42.7	2 250	0.283	645
x 4.8	x 4.78	10.3	0.101	1 310	1.08	28.5	28.8	34.4	1 800	0.288	546
HSS 64x64x6.4	HSS 63.5x63.5x6.35	10.6	0.104	1 350	0.701	22.1	22.8	28.0	1 230	0.232	484
x 4.8	x 4.78	8.35	0.082	1 090	0.593	18.7	22.6	22.9	1 000	0.238	424
x 3.8	x 3.81	6.85	0.067	872	0.506	15.9	24.1	19.2	836	0.241	368
x 3.2	x 3.18	5.82	0.057	741	0.441	13.9	24.4	16.5	717	0.243	323
HSS 51x51x6.4	HSS 50.8x50.8x6.35	8.05	0.079	1 030	0.317	12.5	17.6	16.3	580	0.181	323
x 4.8	x 4.78	6.45	0.063	821	0.278	10.9	18.4	13.8	485	0.187	303
x 3.8	x 3.81	5.33	0.052	679	0.242	9.54	18.9	11.7	410	0.190	271
x 3.2	x 3.18	4.55	0.045	580	0.214	8.42	19.2	10.2	355	0.192	242
x 2.8	x 2.79	4.05	0.040	516	0.194	7.64	19.4	9.15	318	0.194	221
HSS 38x38x4.8	HSS 38.1x38.1x4.78	4.54	0.044	578	0.100	5.27	13.2	6.91	184	0.136	181
x 3.8	x 3.81	3.81	0.037	485	0.091	4.77	13.7	6.04	160	0.139	174
x 3.2	x 3.18	3.28	0.032	418	0.082	4.31	14.0	5.34	141	0.141	161
x 2.5	x 2.54	2.71	0.026	345	0.071	3.71	14.3	4.51	118	0.144	142
HSS 32x32x3.8	HSS 31.8x31.8x3.81	3.06	0.030	389	0.048	3.01	11.1	3.92	87.0	0.114	126
x 3.2	x 3.18	2.65	0.026	338	0.044	2.77	11.4	3.51	77.6	0.116	121
x 2.5	x 2.54	2.20	0.022	281	0.039	2.44	11.7	3.01	66.1	0.118	110
HSS 25x25x3.2	HSS 25.4x25.4x3.18	2.01	0.020	257	0.020	1.56	8.79	2.05	36.3	0.091	80.6
x 2.5	x 2.54	1.69	0.017	216	0.018	1.41	9.12	1.79	31.6	0.093	77.4

STEEL

RECTANGULAR Hollow Structural Sections



METRIC Dimensions and Properties

Designation	Size	Mass	Dead Load	Area	I _x	S _x	r _x	Z _x	I _y	S _y	r _y	Z _y	Torsion J	Shear C _{rt}
mm x mm x mm	mm x mm x mm	kg/m	kN/m	mm ²	10 ⁶ mm ⁴	10 ³ mm ³	mm	10 ³ mm ³	10 ⁶ mm ⁴	10 ³ mm ³	mm	10 ³ mm ³	10 ³ mm ⁴	mm ²
HSS 305x203x13	HSS 305x203x12.7	93.0	0.912	11 800	147	964	111	1 190	78.1	769	81.2	896	167 000	6 450
x 11	x 11.1	82.4	0.808	10 500	132	867	112	1 060	70.5	693	81.9	802	149 000	5 790
x 9.5	x 9.53	71.3	0.699	9 090	116	762	113	925	62.1	611	82.7	701	130 000	5 080
x 8.0	x 7.95	60.1	0.590	7 660	99.4	652	114	787	53.3	524	83.4	596	111 000	4 340
x 6.4	x 6.35	48.6	0.476	6 190	81.5	535	115	640	43.8	431	84.1	486	89 800	3 550
HSS254x152x13	HSS254x152x12.7	72.7	0.713	9 260	75.2	592	90.1	746	33.6	441	60.2	522	78 200	5 160
x 11	x 11.1	64.6	0.634	8 230	68.2	537	91.0	671	30.6	401	61.0	470	70 200	4 660
x 9.5	x 9.53	56.1	0.550	7 150	60.3	475	91.9	589	27.2	357	61.7	413	61 600	4 110
x 8.0	x 7.95	47.5	0.465	6 050	52.0	409	92.7	503	23.5	309	62.4	353	52 600	3 530
x 6.4	x 6.35	38.4	0.377	4 900	42.9	338	93.6	411	19.5	256	63.1	290	43 000	2 900
HSS 203x152x13	HSS 203x152x12.7	62.6	0.614	7 970	43.0	423	73.4	528	27.3	358	58.5	432	56 400	3 870
x 11	x 11.1	55.7	0.547	7 100	39.1	385	74.2	476	24.9	327	59.3	390	50 800	3 530
x 9.5	x 9.53	48.5	0.476	6 180	34.8	343	75.1	419	22.3	292	60.0	344	44 600	3 150
x 8.0	x 7.95	41.1	0.403	5 240	30.2	297	75.9	360	19.3	254	60.7	295	38 200	2 730
x 6.4	x 6.35	33.4	0.327	4 250	25.0	246	76.7	295	16.1	211	61.5	243	31 200	2 260
x 4.8	x 4.78	25.5	0.250	3 250	19.5	192	77.5	228	12.6	165	62.2	188	24 100	1 760
HSS 203x102x13	HSS 203x102x12.7	52.4	0.514	6 680	31.2	307	68.4	405	10.2	201	69.1	186	27 000	3 870
x 11	x 11.1	46.9	0.460	5 970	28.7	282	69.3	367	9.46	186	39.8	224	24 600	3 530
x 9.5	x 9.53	40.9	0.401	5 210	25.8	253	70.3	325	8.56	168	40.5	199	21 900	3 150
x 8.0	x 7.95	34.8	0.341	4 430	22.5	221	71.2	281	7.54	148	41.2	172	18 900	2 730
x 6.4	x 6.35	28.3	0.278	3 610	18.8	185	72.2	232	6.35	125	42.0	143	15 600	2 260
x 4.8	x 4.78	21.7	0.213	2 760	14.7	145	73.1	180	5.03	99.0	42.7	111	12 200	1 760
HSS 178x127x13	HSS 178x127x12.7	52.4	0.514	6 680	26.4	297	62.8	377	15.5	243	48.1	298	33 600	3 230
x 11	x 11.1	46.9	0.460	5 970	24.2	272	63.7	342	14.2	224	48.8	270	30 400	2 970
x 9.5	x 9.53	40.9	0.401	5 210	21.7	244	64.6	303	12.8	202	49.6	240	26 900	2 660
x 8.0	x 7.95	34.8	0.341	4 430	18.9	213	65.4	261	11.2	177	50.3	207	23 100	2 320
x 6.4	x 7.95	28.3	0.278	3 610	15.8	178	66.2	216	9.40	148	51.1	171	19 900	1 820
x 4.8	x 4.78	21.7	0.213	2 760	13.1	164	67.1	167	7.41	117	51.8	133	14 700	1 520
HSS 152x102x11	HSS 152x102x11.1	38.0	0.373	4 840	13.6	179	53.1	230	7.13	140	38.4	172	16 300	2 400
x 9.5	x 9.53	33.3	0.327	4 240	12.4	162	54.0	205	6.50	128	39.1	154	14 500	2 180
x 8.0	x 7.95	28.4	0.279	3 620	10.9	143	54.8	178	5.76	113	39.9	134	12 600	1 920
x 6.4	x 6.35	23.2	0.228	2 960	9.18	121	55.7	148	4.88	96.1	40.6	112	10 500	1 610
x 4.8	x 4.78	17.9	0.175	2 280	7.28	95.6	56.5	116	3.89	76.8	41.3	87.8	8 160	1 270
HSS 127x76x9.5	HSS 127x76.2x9.53	25.7	0.252	3 280	6.12	96.4	43.2	126	2.69	70.5	26.6	87.5	6 800	1 690
x 8.0	x 7.95	22.1	0.217	2 820	5.44	84.4	44.1	111	2.33	62.4	27.2	81.0	5 810	1 400
x 6.4	x 6.35	18.2	0.178	2 320	4.70	74.0	45.5	93.3	2.10	55.1	30.1	65.2	4 890	1 290
x 4.8	x 4.78	14.1	0.138	1 790	3.78	55.9	45.9	73.8	1.70	44.7	30.8	51.7	3 860	1 030
HSS 127x64x5.8	HSS 127x63.5x5.8	23.8	0.234	3 030	5.28	83.2	41.7	112	1.70	53.6	23.7	67.4	4 640	1 690
x 8.0	x 7.95	20.5	0.201	2 610	4.77	75.1	42.7	98.9	1.56	49.1	24.4	60.0	4 130	1 510
x 6.4	x 6.35	16.6	0.166	2 150	4.11	64.8	43.7	83.6	1.36	42.9	25.1	51.0	3 510	1 290
x 4.8	x 4.78	13.1	0.129	1 670	3.33	54.4	44.6	66.1	1.08	35.9	25.9	48.9	3 080	1 090
HSS 127x51x5.8	HSS 127x50.8x5.3	21.9	0.215	2 790	4.45	70.0	39.9	97.7	0.961	37.8	18.6	48.9	2 930	1 690
x 8.0	x 7.95	18.9	0.186	2 410	4.05	63.8	41.0	86.9	0.897	35.3	19.3	44.0	2 650	1 510
x 6.4	x 6.35	15.6	0.153	1 990	3.53	55.5	42.1	73.8	0.798	31.4	20.0	37.9	2 290	1 290
x 4.8	x 4.78	12.2	0.119	1 550	2.87	45.3	43.1	58.9	0.665	26.2	20.7	30.5	1 850	1 030
HSS 102x76x5.8	HSS 102x76.2x5.3	19.1	0.215	2 790	3.41	67.2	35.0	89.6	2.15	56.3	27.7	71.3	4 710	1 210
x 8.0	x 7.95	16.9	0.186	2 410	3.10	61.0	35.8	77.7	1.96	51.4	28.5	63.0	4 170	1 110
x 6.4	x 6.35	13.6	0.153	1 990	2.63	48.5	36.7	71.9	1.52	42.8	25.8	54.5	3 490	1 090
x 4.8	x 4.78	12.2	0.119	1 550	2.18	43.0	37.5	52.5	1.39	36.6	30.0	43.1	2 800	789
HSS 102x51x8.7	HSS 102x50.8x7.95	15.8	0.155	2 010	2.21	43.5	33.2	58.8	0.709	27.9	18.8	35.4	1 950	1 110
x 6.4	x 6.35	13.1	0.129	1 670	1.95	38.4	34.2	50.6	0.638	25.1	19.5	30.7	1 690	968
x 4.8	x 4.78	10.3	0.101	1 310	1.61	31.8	35.1	40.5	0.536	21.1	20.3	24.9	1 370	789
x 3.8	x 3.81	8.37	0.082	1 070	1.36	26.8	35.7	33.9	0.456	18.0	20.7	20.8	1 140	658
x 3.2	x 3.18	7.09	0.090	903	1.09	23.1	35.1	29.0	0.397	15.6	17.1	17.9	940	569
HSS 89x64x8.0	HSS 88.9x63.5x7.95	15.8	0.155	2 010	1.87	42.1	30.5	54.9	1.01	34.3	23.3	43.2	2 450	908
x 6.4	x 6.35	13.1	0.129	1 670	1.65	37.1	31.4	47.1	0.966	30.4	24.0	32.2	2 100	806
x 4.8	x 4.78	10.3	0.101	1 310	1.36	30.6	32.3	38.0	0.803	25.3	24.8	30.1	1 690	667
x 3.8	x 3.81	8.37	0.082	1 070	1.15	25.8	32.8	31.5	0.679	21.4	25.2	25.0	1 400	561
x 3.2	x 3.18	7.09	0.069	903	0.990	22.3	33.1	27.0	0.588	18.5	25.5	21.4	1 190	486
HSS 76x51x8.0	HSS 76.2x50.8x7.95	12.6	0.123	1 600	1.01	26.6	25.1	35.9	0.522	20.5	18.0	26.7	1 270	705
x 6.4	x 6.35	10.4	0.104	1 360	0.917	26.1	31.1	40.0	0.461	18.0	23.5	23.5	1 110	640
x 4.8	x 4.78	8.35	0.082	1 060	0.774	20.3	27.0	25.7	0.407	16.0	19.6	19.3	911	546
x 3.8	x 3.81	6.85	0.067	872	0.660	17.3	27.5	21.6	0.349	13.8	20.0	16.3	762	465
HSS 51x25x3.2	HSS 50.8x25.4x3.18	3.28	0.032	418	0.122	4.81	17.1	6.33	0.040	3.14	9.77	3.84	106	242
x 2.5	x 2.54	2.71	0.026	345	0.105	4.15	17.5	5.35	0.035	2.75	10.1	3.27	89.8	206

Lecture 16 – Blowing in the Wind

Overview:

In addition to loads caused by gravity, which generally act downwards, structures must be designed to resist wind loads which typically act laterally. This chapter presents a simple method for determining the loads caused by severe windstorms and outlines a procedure for designing cross bracing to safely resist them.

Wind Loads

A strong wind is capable of producing forces that are large enough to cause structures to collapse, like the trees shown in Fig. 16.1 and the bridge over the Firth of Tay shown in Fig. 16.2. The bridge collapsed in 1879 when a train attempted to cross over it during winds blowing at speeds of up to 117 km/h, killing all 75 passengers on board. In regions of low seismicity, wind loads are usually the most important lateral load which structural engineers must consider when designing structures.

When a wind is blowing onto a surface of a body, it applies a force, F_{wind} , which can be calculated using Newton's drag equation:

$$F_{wind} = \frac{1}{2} \rho v^2 c_D A \quad (16.1)$$

In Eq. (16.1), ρ is the density of the fluid, v is its velocity, A is the frontal area on which the wind acts, and c_D is a drag coefficient which describes the ability of the wind to travel around the body. c_D may take on a range of values, being 0.2 for a well-designed sports car, 0.75 for a sphere or cylinder, and 1.5 for boxy objects like a cube or a wall.

A simple design value of the wind pressure, w_{wind} , can be obtained by using the density of air, $\rho = 1.2 \text{ kg/m}^3$, and assuming appropriately conservative values for v and c_D . If the maximum wind speed is assumed to be 170 km/h and c_D is taken as 1.5, the wind pressure is equal to:

$$w_{wind} = \frac{F_{wind}}{A} = 2.0 \text{ kPa} \quad (16.2)$$

Therefore, an appropriate value for design is $w_{wind} = 2.0 \text{ kPa}$ of force, acting horizontally on the structure.

Design of Cross Bracing to Resist Wind Loads

To prevent the main trusses of a bridge from collapsing due to the force of the wind, cross bracing must be provided to connect the top chords and bottom chords together. With this bracing, the bridge will then be able to transfer the applied wind forces to the supports on the ends, in a similar way that the main trusses support the gravity loads applied to the deck and transfer them to the supports. A typical arrangement for the top and bottom braces is shown in Fig. 16.3.



Fig. 16.1 – Pine trees broken by a windstorm



Fig. 16.2 – Firth of Tay Bridge, 29 December 1879. The engineer, Sir Thomas Bouch, was unable to produce the wind calculations during the subsequent investigation.

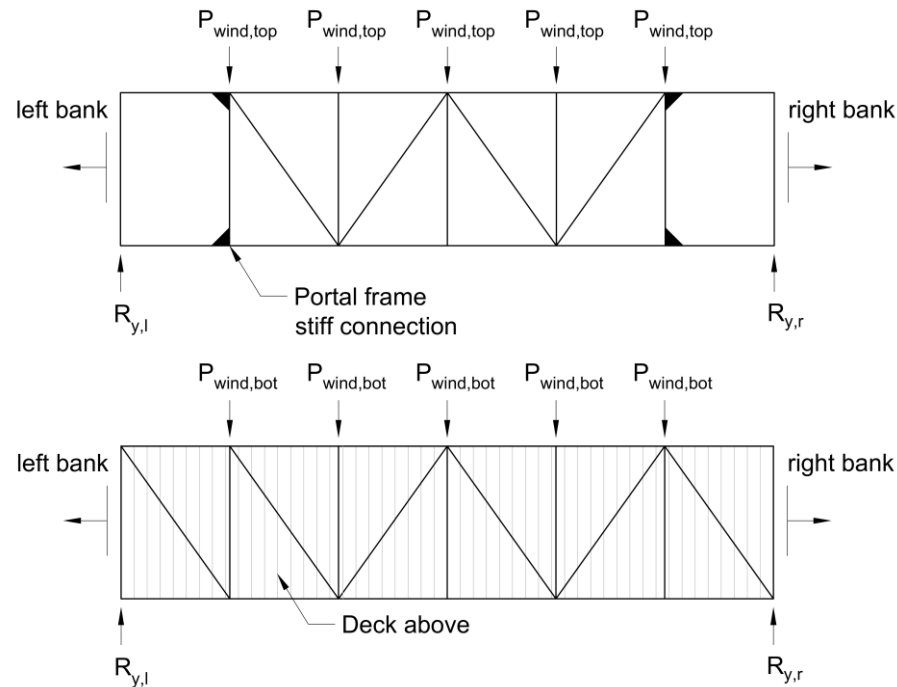


Fig. 16.3 – Arrangement of cross bracing on the top (above) and bottom (below) of a truss bridge. The bridge has the same geometry as the one analyzed in Lecture 13.

In each of the schematics shown in Fig. 16.3, P_{wind} is the joint load caused by the wind blowing onto the side of the bridge. Because the direction of the wind is not fixed, the cross bracing must be designed to resist loads acting on either side. Furthermore, the loads can push towards the bridge, or pull away due to suction effects. This results in four possible combinations of loading which must be considered when designing the members.

Determining the forces in the bottom cross bracing follows the same process as the analysis of the main truss for gravity loads. First, the reaction forces $R_{y,l}$ and $R_{y,r}$ must be determined based on the applied loads. After these loads have been determined, the forces in the braces can be obtained by using the Method of Joints or Method of Sections.

Analyzing the top cross bracing using a truss analysis method like the Method of Joints is not immediately possible due to the lack of diagonal members which connect the supports to the rest of the braces. These members are omitted to allow entry and egress of the bridge. In lieu of these members, the connection is typically stiffened to allow the forces in the cross bracing to be transferred to the ground.

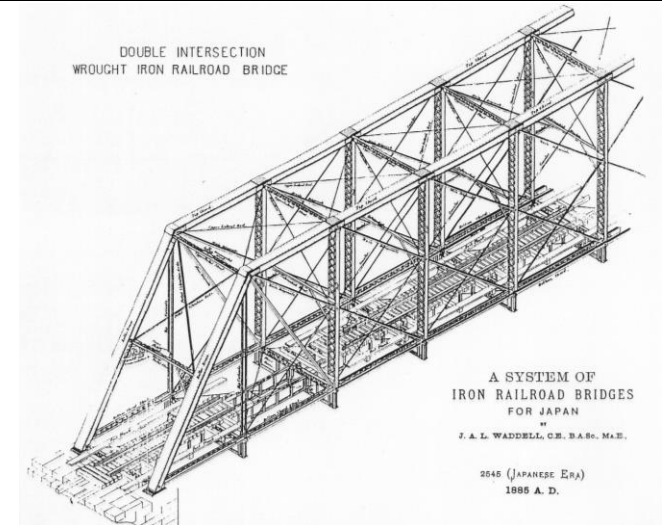


Fig. 16.4 – Isometric view of a truss railway bridge. Note the use of stiff connections at the front to eliminate the need for a brace crossing over this region. The open entryway stiffened at the corners is called a **Portal Frame**.

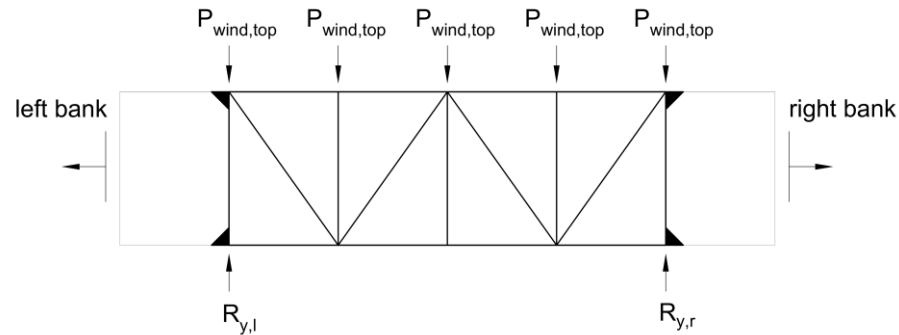


Fig. 16.5 – Analysis of the forces in the top braces

Fig. 16.5 shows a simplified approach to solving for the forces in the top braces. In this schematic, we have assumed that the reaction forces provided at the supports can be transferred along the outside members to meet the braces. With this assumption, the brace forces can now be determined using the Method of Joints.

Calculating Joint Loads using the Tributary Area

Although calculating the brace forces once the wind loads have been determined is a straightforward task, obtaining the joint loads caused by the wind requires a series of intricate calculations to be done. The joint load P_{wind} is calculated in a similar way as the joint loads caused by gravity, but instead the loads act on the frontal area of the bridge, $A_{frontal}$, instead of on the deck:

$$P_{wind} = w_{wind} A_{frontal} \quad (16.3)$$

In Eq. (16.3), w_{wind} is typically taken as 2.0 kPa.

When determining the frontal area, the tributary area concept is used in the same way it was used for obtaining the gravity loads, meaning that a joint is responsible for carrying the loads applied to the surfaces halfway to each of its surrounding neighbours. The frontal area used in Eq. (16.3) is hence the solid area within this tributary zone.

Fig. 16.6 show the elevation view of a truss bridge and illustrates how the wind pressure is distributed to produce discrete loads applied to the joints. The frontal area associated with joint A is all of the solid area within Zone A, and likewise for joint B. Due to the presence of the handrail in Zone B, the force applied to joint B will greatly exceed what joint A must carry.

Note: Moving the reaction force from the support to the top bracing requires a carefully designed connection. The design of these connections is outside of the scope of CIV102 but can pose a serious design challenge in real-life engineering practice.

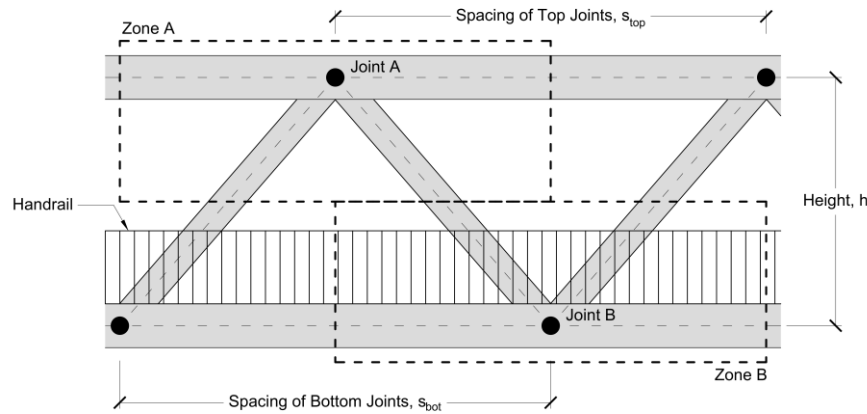


Fig. 16.6 – Elevation view of a truss bridge. Joint A is responsible for carrying the loads applied to the solid surfaces within Zone A, and joint B is responsible for carrying the loads applied to the solid surfaces in Zone B.

Fig. 16.7 shows the details of Zone A and B in more detail. Each zone has a height of $h/2$, and a width of s_{top} and s_{bot} respectively. The frontal area in Zone A can be approximated using the following equation:

$$A_{frontal} \cong \sum_{i=1}^n b_i l_i = b_1 l_1 + b_2 l_2 + b_3 l_3 + b_4 l_4 \quad (16.4)$$

In Eq. (16.4), n is the number of members within the zone, b_i is the outside dimension of the cross section facing the wind, and l_i is the length of the member within the zone.

For situations involve a handrail, like in Zone B in Fig. 16.7, the frontal area of the handrail is much larger than the frontal area of the HSS, which can hence be neglected for simplicity. Although the handrail may consist of closely spaced vertical members with gaps in between, the resulting turbulence as the air flows through these narrow spaces will increase the drag force applied to the railing. Therefore, the handrail may be approximated as a solid surface, resulting in a frontal area of:

$$A_{frontal} \cong h_{rail} s_{bot} \quad (16.5)$$

Note that Eq. (16.4) and (16.5) should be modified when used in situations where the horizontal or vertical spacing of the joints is irregular. The governing principle when making these modifications is that each joint is responsible for the zone halfway to each of its neighbours.

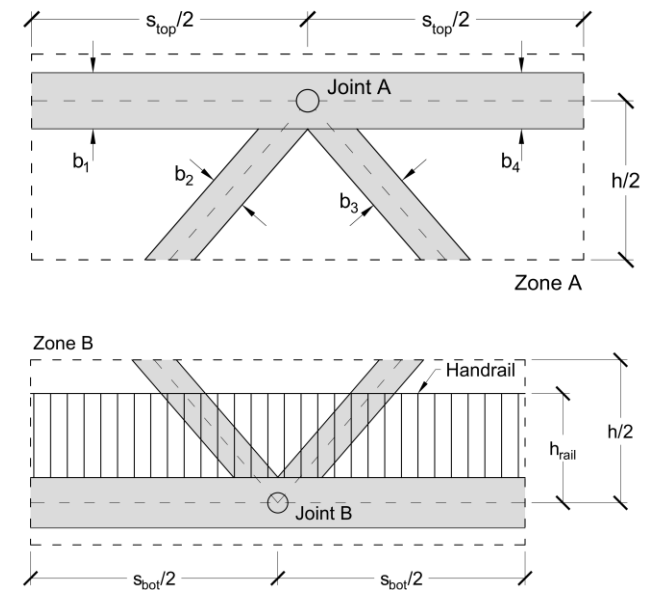


Fig. 16.7 – Schematics for determining the tributary areas in Zone A and Zone B.

Lecture 17 – A Bracing Lecture

Overview:

In this chapter, the process of designing cross braces to laterally support members in compression is presented. Compression members typically tend to deform because of imperfect alignment, which can reduce their buckling strength if their joints are not adequately restrained from moving. A simple analysis technique is derived to ensure that the lateral movements at any joint does not exceed 1% of the attached member's length.

Stability and Misalignment of Compression Members

Consider the truss bridge shown in Fig. 17.1, whose top chord is in compression as it supports a substantial gravity load applied to the deck. When designing the chord, it was assumed that the member and its joints were perfectly aligned so that the compression member buckled between the joints with an effective buckling length equal to the spacing between the joints (i.e. L = the joint spacing) when evaluating the buckling force P_{crit} .

Recall: Gravity loads are applied to the deck, and include the weight of the deck itself, the weight of the structural components, and the weight of a large crowd of people.

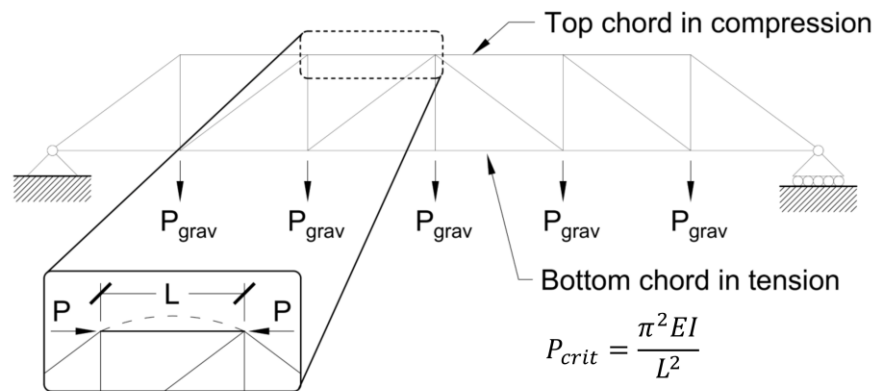


Fig. 17.1 – Design of top chords against buckling using the joint spacing, L

In reality, these assumptions are generally not true: the members will be slightly misaligned due to the imperfect nature of construction, and the stability of the joints will depend on the stiffness of the braces used to connect the chords of the truss together. In extreme cases, like truss bridge in Fig. 17.2 which does not contain any diagonal braces connecting its top chords together, the compression chords will buckle over the entire length of the bridge at a much lower load than originally anticipated.

The bridge shown on the right in Fig. 17.2, which contains diagonal braces and rigid connections at the portal frame, avoids this issue by preventing the joints from deforming in the out-of-plane direction. Having this bracing system provides stability to the structure and allows us to design the compression members using our original assumption that the effective buckling length is the joint spacing. The braces which connect these compression members must therefore be sized so that they can provide an adequate restraining force to prevent the chord from buckling at its joints.

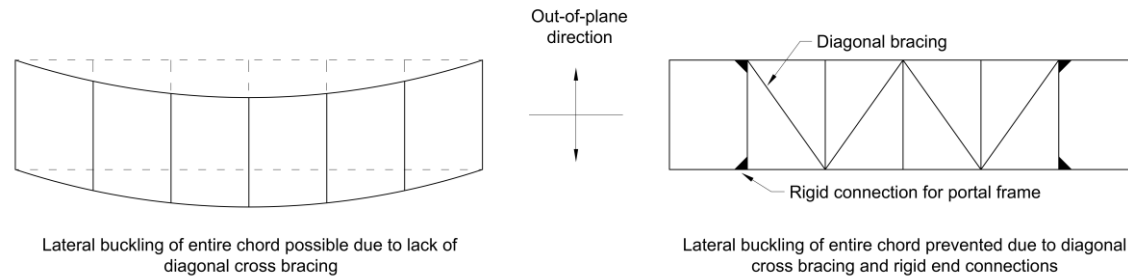


Fig. 17.2 – View of a truss bridge from above, showing how cross bracing can restrain the chords from buckling over the entire span.

Design Check for Stability

Fig. 17.3 shows two schematics of a compression member with a length of $2L$ and subjected to a compression force of P . Because the joint at the midspan is not restrained, it buckles and displaces laterally at its midspan by a distance Δ . To prevent the system from deforming further, a restraining force, R , is required to pull the displaced joint back to its original position; this is shown in the second drawing in the figure.

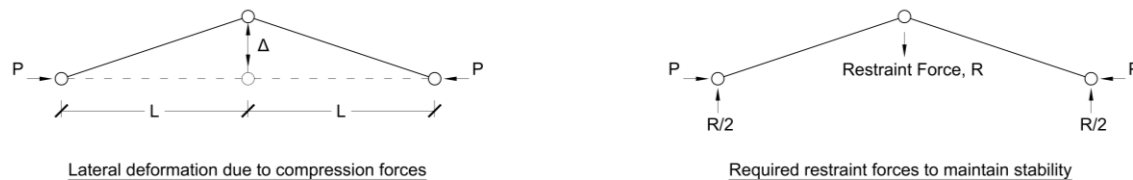


Fig. 17.3 – Analysis of a compression member as the joint moves out of plane

The required restraint force to restore the joint back into its original position depends on how much it has displaced, i.e. as the deformation Δ increases, R must increase as well. In design, an appropriate value of Δ to use is $\Delta = 0.01L$ (1% of L). This misalignment, equal to 1% of the length of the individual members, is a reasonable upper bound of what can be expected given modern construction practices.

Fig. 17.4 shows a free body diagram of half of the situation shown in Fig. 17.3. Because the system is in equilibrium, taking moments about the bottom left joint results in the following equation:

$$P \times \Delta = \frac{R}{2} \times L \quad (17.1)$$

Substituting the requirement that $\Delta = 0.01L$ results in the following requirement for the restraint force:

$$R = 0.02P \quad (17.2)$$

Therefore, to ensure that the compression member is adequately braced for stability, there must be braces attached to each of its joints which are able to provide a local restraining force of $R = 0.02P$.

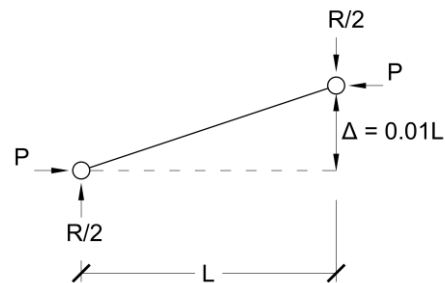


Fig. 17.4 – Free body diagram used to determine the required restraining force, R , if $\Delta = 0.01L$

Fig. 17.5 shows how the diagonal braces are able to provide the required restraining force as the intermediate joint moves laterally. As the joint displaces outwards, the two diagonal braces come into tension and pull the joint back to its original position. To maintain vertical equilibrium at the bottom joints, the vertical members must go into compression, which in turn stabilizes the top joints by providing the reaction forces shown in Fig. 17.3. The opposite occurs if the intermediate joint was to instead displace inwards.

Just like when designing for wind, the braces supporting compression members must also be designed for four possible situations because either of the compression chords may buckle towards or away from the centre of the bridge. These four situations are illustrated in Fig. 17.6, which shows a portion of the braces connecting the top chords from plan view.

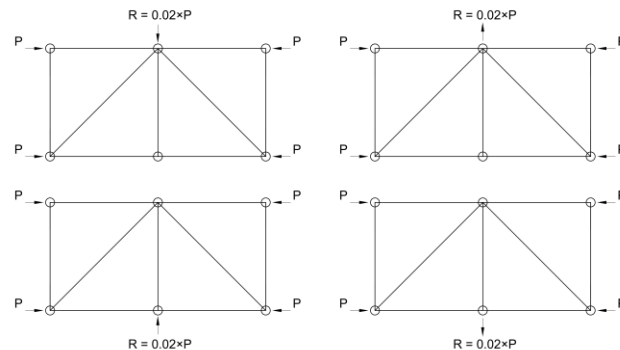


Fig. 17.6 – Summary of design cases when designing braces for stability

It should be emphasized that the stability design described above is a **local** check to ensure that each joint is adequately supported by the braces. This contrasts with a **global** analysis, which is done when designing for wind for example, which involves obtaining the reaction forces and complete member forces for the entire bridge.

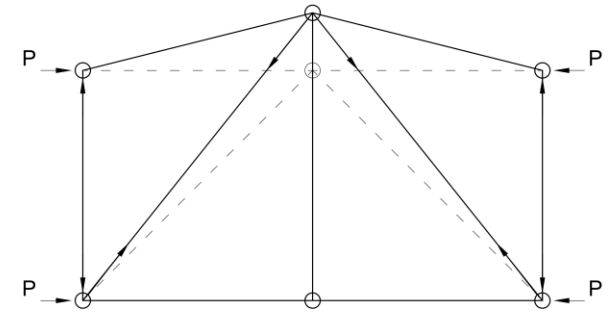


Fig. 17.5 – Mechanism by which cross bracing restrains joints from buckling outwards

Design Process for Cross Bracing

The design of the braces on the top and bottom of the bridge to resist wind loads and instability effects can be done together once the main trusses have been designed to resist the gravity loads. The braces which connect the bottom chord will typically only need to be designed to resist wind loads because the gravity loads cause them to go into tension. This contrasts with the design of the braces on the top of the bridge, which must resist wind loads and provide stability when the gravity loads cause the top chords to carry significant amounts of compression.

To design the top braces, the following steps should be followed:

1. Calculate the wind loads and determine the brace forces. This is a global analysis which involves solving for the reaction forces and then obtaining the brace forces by using the Method of Joints or Method of Sections.

2. Calculate the forces in the braces which are required to stabilize the compression chords under gravity loads. Using the forces in the chords as obtained under gravity loads, calculate the required restraint force needed to support the joints along the top chord from displacing laterally. This is done by performing a series of local analyses, like the ones shown in Fig. 17.6, with the goal of calculating the forces in the members directly attached to the displaced joint.

3. Select appropriate HSS sections which can carry the larger of the forces obtained in steps 1 and 2. The braces should be designed for both tension and compression because the wind or instability can act in any direction. Typically, only one or two HSS sizes are used for the braces to avoid errors during construction and avoid potential supply issues.

The design process for the bottom braces is identical but omits step 2 because the bottom chords will not buckle under the tension forces caused by gravity loads.

Note: The compression force in the top chord varies along its length. If you find when drawing a schematic like those in Fig. 17.6 that the forces in the chords on the two sides are not equal, use the larger value to find R to be conservative.

Note: The braces need to be designed for the more severe case of wind or instability, but not both at the same time. This is because the loads will not occur at the same time. For example, during the event of a severe windstorm, it is highly unlikely for a large crowd of people to occupying the bridge at the same time. High wind loads will occur in the absence of high gravity loads, and vice-versa.

Lecture 18 – Method of Virtual Work

Overview:

Although determining the forces in a truss bridge structure is a straightforward task, determining the deflection of a loaded structure can be an arduous challenge. In this chapter, the Method of Virtual Work is presented, which transforms the task of solving displacements from a complex geometric problem to a simple statics problem.

Introduction

In structural engineering, it is equally important for a structure to have adequate strength and stiffness. The importance of strength, which is the ability of a structure to safely carry the expected loads, has been discussed extensively in previous chapters. Stiffness on the other hand is a measure of how well a structure can limit its deformations under service loads. Excessive deformations can disrupt other functions of the structure and are generally unpleasant if they are large enough to be observed by users of the structure.

Determining the deformations of a truss structure when loaded can be done by solving for the forces in the members, calculating the corresponding changes in length of all of the members, and then determining the displaced shape using these new member lengths. Although this is a feasible procedure to determine the deflections of very simple structures, it quickly becomes impractical as the number of members which need to be considered increases.

An alternative means of solving for the displacements uses energy methods. According to the theorem of conservation of energy, the work done by the externally applied loads \mathbf{F} acting over the external displacements Δ , W_{ext} , must equal to the work done by the internal members changing length, $\Delta\mathbf{l}$, while carrying internal forces \mathbf{P} , \mathbf{W}_{int} . In the case where \mathbf{m} loads which are applied to a truss structure with \mathbf{n} members, this can be expressed as:

$$W_{\text{ext}} = W_{\text{int}} \quad (18.1)$$

The work terms in Eq. (18.1) can be expanded further, which results in the following:

$$\sum_{i=1}^m \int F_i d\Delta_i = \sum_{j=1}^n \int P_j d\Delta_l_j \quad (18.2)$$

Note: The integrals in Eq. (18.2), which represent the work done by the forces acting over displacements, are a mathematical representation of the area under a force-displacement curve. Refer to Lecture 6 for more information.

The equivalence of the external work and internal work is the basis of the **Method of Virtual Work**.

The Method of Virtual Work: Derivation

To introduce the Method of Virtual work, consider the simple two-member truss which is shown in Fig. 18.1. There is a force \mathbf{F} applied to the structure which causes joint B to translate horizontally and vertically by ΔB_x and ΔB_y respectively. The two members, member AB and BC, will resist the applied force by carrying internal member forces, \mathbf{P}_{AB} and \mathbf{P}_{BC} respectively, and will stretch or contract by $\Delta\mathbf{l}_{\text{AB}}$ and $\Delta\mathbf{l}_{\text{BC}}$ as a result. The quantity which we would like to solve is the vertical displacement of point B.

Note: The derivation of the method of virtual work is included here for completeness but will not be assessed during the course. You will be assessed based on how well you are able to apply the method to solve problems.

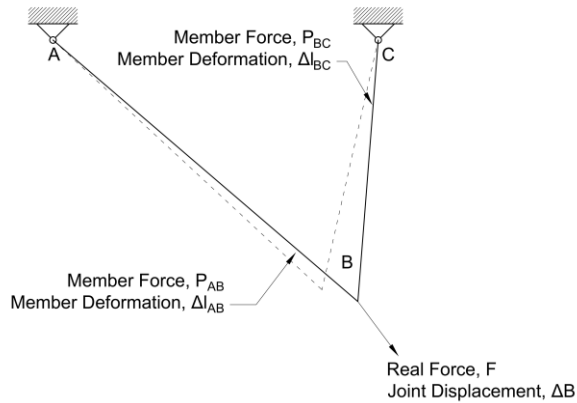


Fig. 18.1 – Real system of forces and displacements

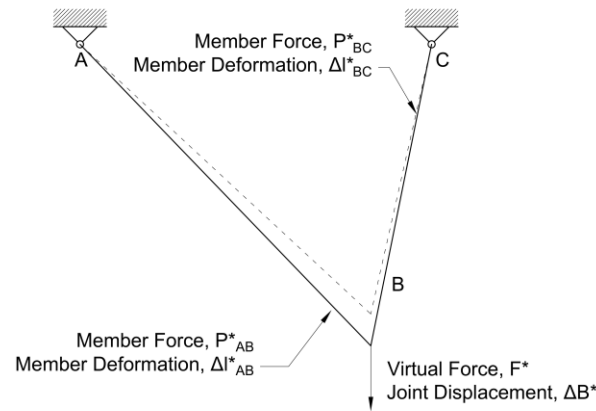


Fig. 18.2 – Virtual system of forces and displacements

Consider the equivalence of the external work done by the force \mathbf{F} as it acts over the displacements at joint B and the internal work done by the members as they deformed in response to the applied load. If it is assumed that all of the members are linear elastic, then Eq. (18.2) can be rewritten as:

$$\sum_{i=1}^m \frac{1}{2} F_i \Delta_i = \sum_{j=1}^n \frac{1}{2} P_j \Delta l_j \quad (18.3)$$

Expanding Eq. (18.3) for our simple system and breaking up \mathbf{F} into its x- and y- components yields:

$$\frac{1}{2} F_x \Delta B_x + \frac{1}{2} F_y \Delta B_y = \frac{1}{2} P_{AB} \Delta l_{AB} + \frac{1}{2} P_{BC} \Delta l_{BC} \quad (18.4)$$

The terms on the right side of Eq. (18.4), which contain the internal forces and the changes in lengths of the members, can be solved using tools discussed in the previous chapters. However, the left side of our equation contains two unknown displacements, ΔB_x and ΔB_y , which cannot be solved because we only have one equation.

To overcome this issue, we will introduce a **virtual system**, shown in Fig. 18.2, which is geometrically identical as the original system, but only contains a **virtual force**, \mathbf{F}^* which acts in the same position and direction of our displacement of interest, ΔB_y . The virtual force causes the system to have virtual member forces, \mathbf{P}^*_{AB} and \mathbf{P}^*_{BC} which result in virtual member deformations, Δl^*_{AB} and Δl^*_{BC} , and virtual displacements at joint B, ΔB^*_x and ΔB^*_y . Writing the work equation for this system, noting that the x-component of \mathbf{F}^* is equal to zero, results in:

$$\frac{1}{2} F^* \Delta B^*_y = \frac{1}{2} P^*_{AB} \Delta l^*_{AB} + \frac{1}{2} P^*_{BC} \Delta l^*_{BC} \quad (18.5)$$

Note: The virtual force F^ has an arbitrary magnitude and is usually taken as $F^* = 1$ kN. The key concept when specifying F^* is that \mathbf{F}^* has the same location and orientation as the displacement of interest. F^* is sometimes called a dummy load.*

Eq. (18.5) contains the products of virtual forces and virtual displacements, which are unrelated to the real forces and real displacements which we are interested in. If we take advantage of the fact that the structure is linear elastic, then we can combine our virtual system with our real system, resulting in a hybrid system which has both real and virtual forces and real and virtual displacements. This is shown in Fig. 18.3.

Note: The net forces, stresses and strains resulting from the real load F and virtual force F^ acting together is simply the sum of the effects caused by each individual force. This is called the **Superposition Property** (sometimes referred to as the **Superposition Principle**) and is applicable to any linear elastic system.*

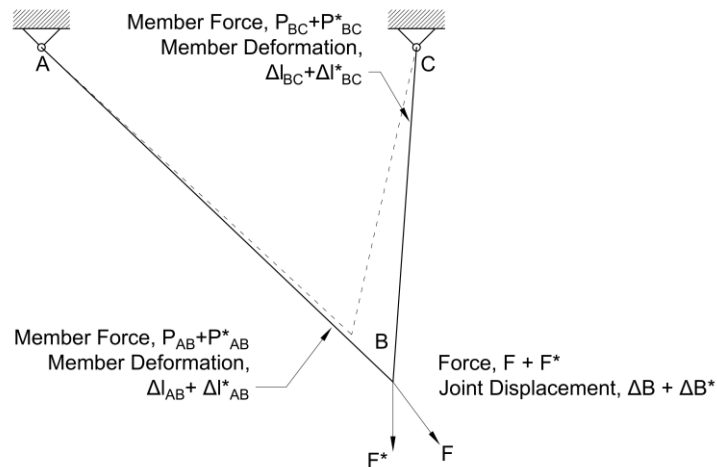


Fig. 18.3 – Hybrid system containing both real and virtual quantities

Fig. 18.4 contains four plots which show the force-displacement relationships of the structure and its members due to the application of both the real and virtual forces. The top two plots show the relationships between the externally applied forces and the displacements of joint B, and the bottom two plots show the relationships between the internal member forces and their member deformations. The area underneath the curves represent the work done; the red areas correspond to work done by the real forces acting over the real displacements, and the blue areas represent the work done by the virtual forces acting over the virtual displacements.

By using the principle of equivalent internal and external work in Eq. (18.1), the area underneath the top two graphs, the external work, is equal to the area underneath the bottom two graphs. Furthermore, the red areas in the top graphs must equal the red areas in the bottom graphs, due to Eq. (18.4), and the blue areas in the top graphs must also equal the blue areas in the bottom graphs, due to Eq. (18.5).

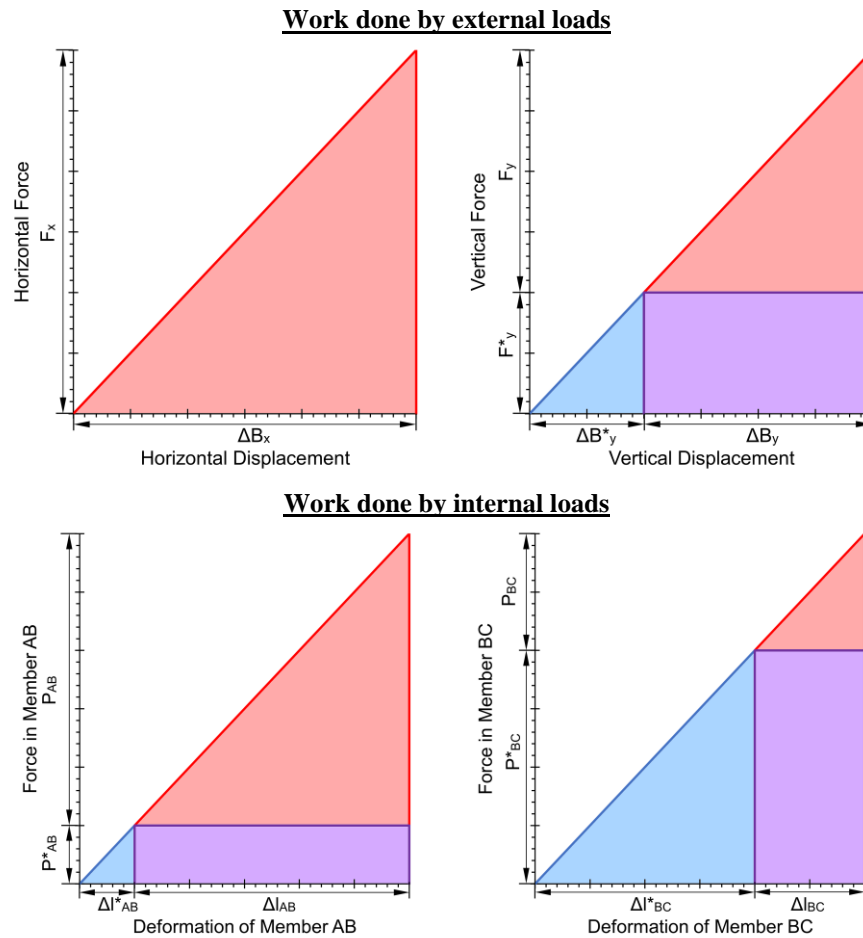


Fig. 18.4 – Load-displacement plots for the structure (top) and individual members (bottom) when subjected to a real load F and a virtual load F^* . The area underneath each curve is equal to the work done.

Because the total areas, as well as the red and blue areas, must equal, it can also be concluded that the area of the purple regions, which are the product of a virtual force and a real displacement, must equal as well. These areas represent the **virtual work** done by the virtual forces, F^* , P_{AB}^* and P_{BC}^* acting over the real displacements, ΔB_y , Δl_{AB} and Δl_{BC} . Expressing this equivalence mathematically results in the following equation:

$$F^* \Delta B_y = P_{AB}^* \Delta l_{AB} + P_{BC}^* \Delta l_{BC} \quad (18.5)$$

Note: The terms in Eq. (18.5) do not have a coefficient of $\frac{1}{2}$ because they represent the rectangular areas under the load-displacement relationships.

In Eq. (18.5), there is now only one unknown displacement, $\Delta \mathbf{B}_y$, which can be solved once the other terms are found from statics and Hooke's law. The advance of using the Method of Virtual work is that by using a virtual system which contains one load, we are always able to obtain single equation with one unknown variable, regardless of the size of the structure and complexity of the real loads. Therefore, Eq. (18.5) can be generalized for a system of arbitrary complexity to be:

$$F^* \Delta = \sum_{i=1}^n P_i^* \Delta l_i \quad (18.6)$$

Note: When using Eq. (18.6), the product of a force and displacement will be in Joules if the force is in kN and the displacement is in mm. Furthermore, the sign of the virtual work is important, as a compressive force acting over a tensile deformation produces negative work as does an upwards external force acting over a downwards displacement (and vice versa).

Where the variables in Eq. (18.6) are defined as follows:

- Δ is a real joint displacement of interest.
- F^* is a virtual load of arbitrary value (usually taken as 1 kN) applied to the structure which has the same location and direction as Δ .
- P_i^* are the virtual member forces resulting from the virtual force F^* .
- Δl_i are the real member deformations caused by the real forces in the system.
- n is the total number of members in the truss structure.

The Method of Virtual Work: Summary and Example

The basic procedure to use the method of virtual work is shown below:

1. Solve for all of the member forces, P_i , due to the real loads using any analysis method.
2. Using the member properties and the real member forces, calculate the real member deformations Δl_i .
3. Identify the displacement of interest, Δ .
4. Create a separate virtual system with a single virtual load, F^* , which has the same location and direction as Δ .
5. Solve for the virtual member forces, P_i^* .
6. Use Eq. (18.6) and solve for Δ .

To illustrate this process, consider the truss bridge shown below in Fig. 18.5 whose member forces are the result of the real applied loads.

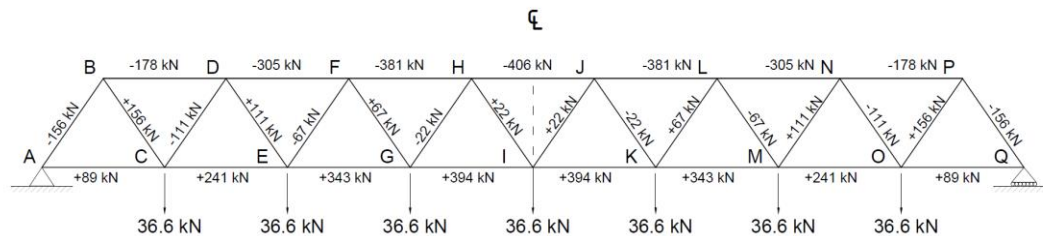


Fig. 18.5 – Real member forces. Note that each horizontal member is 3.75 m long and each diagonal member is 3.29 m long.

If the deflection of the bridge at the midspan is required, a separate virtual system consisting of a single point load applied downwards at the centre of the bridge will be used. This virtual system, including the resulting virtual member forces, is shown in Fig. 18.6.

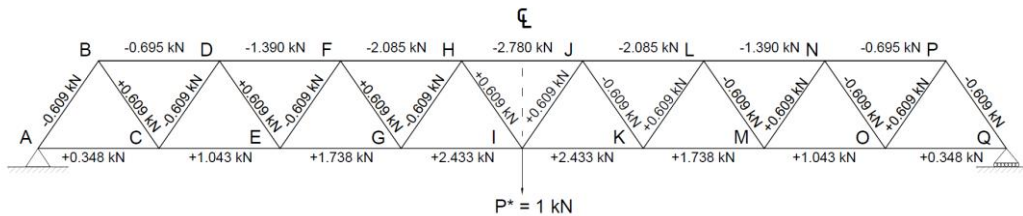


Fig. 18.6 – Virtual system of forces caused by a 1 kN load at the midspan

Performing the calculations when applying Eq. (18.6) to a large system is commonly done using a large table, like the one shown in Fig. 18.7. The column on the far right, which contains the virtual work, is the product of the calculated member deformations, Δ , and the virtual member forces \mathbf{P}^* . By summing over the sixteen members in the table and multiplying by two (to account for the work done by the sixteen members on the other side of the bridge), the total internal work done was found to be 64.74 J. Equating this value to the external work and dividing by the 1 kN virtual load results in a calculated deflection of 68.7 mm downwards.

103_u

Member	Force P kN	Area A mm ²	Stress σ MPa	Strain ϵ mm/m	Length L m	Deform. Δ mm	Dummy Force kN P*	Work J
BD	-178	2760	-64.4	-0.322	3.75	-1.208	-0.695	0.840
DF	-305		-110.4	-0.552	3.75	-2.07	-1.390	2.877
FH	-381		-138.0	-0.690	3.75	-2.59	-2.085	5.400
HJ	-406		-147.2	-0.736	1.875	-1.380	-2.780	3.836
AC	+89	2280	+39.0	+0.195	3.75	+0.731	+0.348	0.254
CE	+241		+105.8	+0.529	3.75	+1.984	+1.043	2.069
EG	+343		+150.4	+0.752	3.75	+2.820	+1.738	4.901
GI	+394		+172.6	+0.863	3.75	+3.236	+2.433	7.873
AB	-156	1790	-87.0	-0.435	3.29	-1.430	-0.609	0.871
CD	-111	1790	-62.2	-0.311	3.29	-1.022	-0.609	0.622
EF	-67	1550	-43.1	-0.216	3.29	-0.708	-0.609	0.431
GH	-22	1550	-14.4	-0.072	3.29	-0.237	-0.609	0.144
BC	+156	1060	+147.0	+0.735	3.29	+2.416	+0.609	1.471
DE	+111	1060	+105.0	+0.525	3.29	+1.726	+0.609	1.051
FG	+67	516	+129.5	+0.648	3.29	+2.128	+0.609	1.296
HI	+22	516	+43.2	+0.216	3.29	+0.710	+0.609	0.432

$\Sigma = 34.37$

Total internal work = $2 \times 34.37 = 68.74$ Joules

Total external work = $1 \times \Delta_I \therefore \Delta_T = \underline{68.7 \text{ mm}}$

Fig. 18.7 – Summary of calculations to obtain the midspan deflection of a truss bridge

Lecture 19 – Where Have All the Soldiers Gone?

Overview:

Several types of loading, such as a moving crowd of people, a windstorm, or an earthquake, apply dynamic loads to structures. Dynamic loads, unlike static loads, vary in time, and may produce resonant effects which can magnify the stresses and deflections experienced by the structure. In this chapter, a simple method to consider dynamic effects in linear elastic structures is introduced.

Free Vibration

As noted in Lecture 7, the behaviour of a simple spring-mass system is governed by the following differential equation:

$$m \frac{d^2 x(t)}{dt^2} + kx(t) = 0 \quad (19.1)$$

Where $\mathbf{x(t)}$ is a time-varying function describing the displacement of the mass, \mathbf{m} is the mass, and \mathbf{k} is the axial stiffness of the spring. Solving Eq. (19.1) for a system which vibrates vertically results in a sinusoidal function with amplitude \mathbf{A} , natural frequency ω_n and phase shift ϕ which oscillates around the static displacement of the mass under the force of gravity, Δ_o :

$$x(t) = A \sin(\omega_n t + \phi) + \Delta_o \quad (19.2)$$

The response described by Eq. (19.2) is shown in Fig. (19.1). Note that in this idealized system, there is no loss of energy and the mass will continue to oscillate until it is interrupted by an external action.

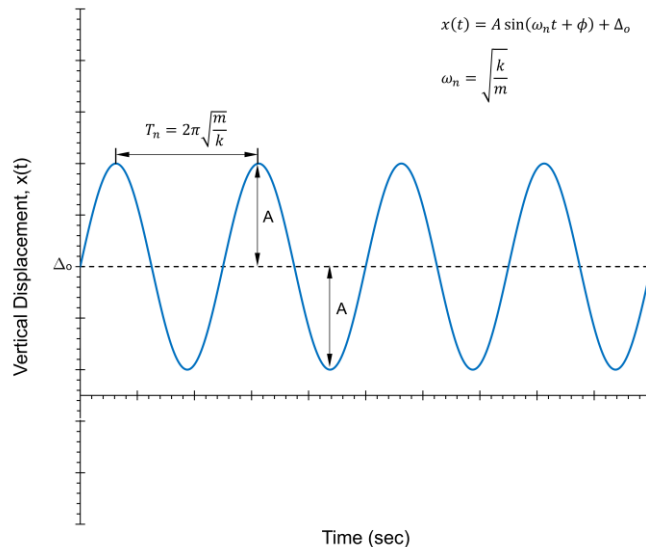


Fig. 19.1 – Undamped free vibration

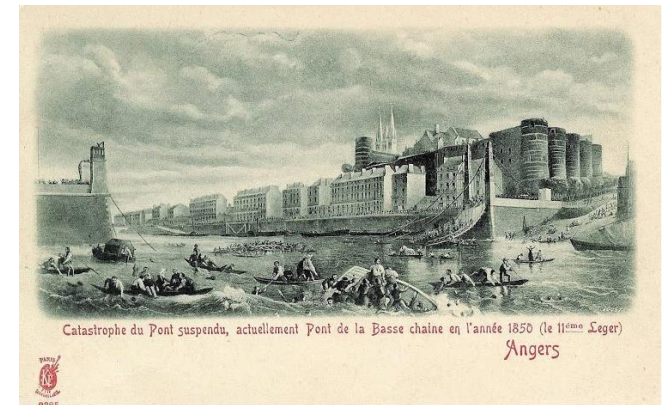


Fig. 19.1 – Collapse of the Angers Bridge in France in 1850. The bridge collapsed as a battalion of soldiers was marching across, leading to 226 deaths.

*Note: A system undergoing free vibration is sometimes referred to as a **Simple Harmonic Oscillator***

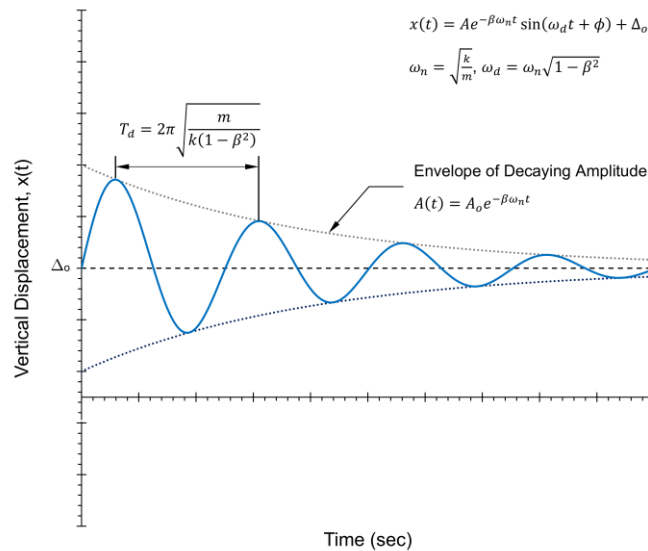


Fig. 19.2 – Damped free vibration

Damped Free Vibrations

In reality, vibrating systems will gradually come to rest due to energy being dissipated by friction or other effects. This gradual loss of energy in a vibrating system is caused by **damping**, which can be an engineered feature or an inherent property of the system. The damping in a system is quantified by the **damping ratio**, β , which is the ratio between the provided damping properties of the system and the minimum amount of damping needed to prevent the system from oscillating.

The differential equation for freely vibrating systems which have damping is a slightly modified version of Eq. (19.1):

$$m \frac{d^2 x(t)}{dt^2} + 2\beta\sqrt{mk} \frac{dx(t)}{dt} + kx(t) = 0 \quad (19.3)$$

The solution to this differential equation is a sinusoidal function like the solution to Eq. (19.3), but has an amplitude which decays to zero exponentially:

$$x(t) = Ae^{-\beta\omega_n t} \sin(\omega_d t + \phi) + \Delta_o \quad (19.4)$$

In Eq. (19.4), ω_d is the damped frequency which has units of rad/s. It is related to the natural frequency, ω_n , by the following equation:

$$\omega_d = \omega_n \sqrt{1 - \beta^2} \quad (19.5)$$

Note: In civil structures, typical values of β range from 0 to 0.05 (5%). Mechanical systems, like vehicles or other equipment, may have damping ratios which are 1.0 or greater.

Note: The derivation of the differential equation and its solution are beyond the scope of CIV102. This material will be covered in future physics and dynamics courses.

In civil structures, the value of β is usually very low, resulting in ω_d being essentially the same as ω_n . The response described by Eq. (19.4) is shown in Fig. (19.2), where it can be seen that the amplitude of vibration gradually dies out and the mass eventually settles at $x = \Delta_o$.

Forced Oscillation

In the previous scenarios, the spring-mass system was freely vibrating without the influence of an externally applied dynamic load. In reality, structures may be subjected to dynamic loading due to the movement of people crossing over a bridge or the vibrations caused by an earthquake. The simplest form of dynamic loading is when the system is subjected to harmonic or sinusoidal load with amplitude F_o and loading frequency ω in rad/sec (or f in cycles per second):

$$F(t) = F_o \sin \omega t \quad (19.6)$$

Substituting this loading into the dynamic equilibrium equation for a damped oscillator results in the following differential equation:

$$m \frac{d^2 x(t)}{dt^2} + 2\beta \sqrt{mk} \frac{dx(t)}{dt} + kx(t) = F_o \sin \omega t \quad (19.7)$$

The complete solution to Eq. (19.7) is complex and beyond the scope of CIV102. It is composed of two parts: a **transient** component, which describes the behaviour shortly after the loading is first applied, and a **steady state** component, which describes the response of the system after it has settled into a rhythmic pattern. The steady state solution, which is particularly relevant for design, is shown below:

$$x(t) = DAF \times \frac{F_o}{k} \sin(\omega t + \phi) + \Delta_o \quad (19.8)$$

In Eq. (19.8), the **DAF** is a **Dynamic Amplification Factor**, which is calculated as:

$$DAF = \frac{1}{\sqrt{\left(1 - \left(\frac{f}{f_n}\right)^2\right)^2 + \left(\frac{2\beta f}{f_n}\right)^2}} \quad (19.9)$$

The response of a vibrating system when subjected to time-varying loads is strongly influenced by the ratio of the driving frequency, f , and the natural frequency of the system, f_n , as it influences both the frequency of the resulting displacement and the amplitude of the response through the DAF. To illustrate this, Fig. 19.3 shows the response of a system when subjected to the same load but at different frequencies. The plot on the left shows a minor reduction in amplitude for a driving frequency which is much higher than the natural frequency, while the plot on the right shows a major increase in amplitude when the driving frequency is about half of the natural frequency.

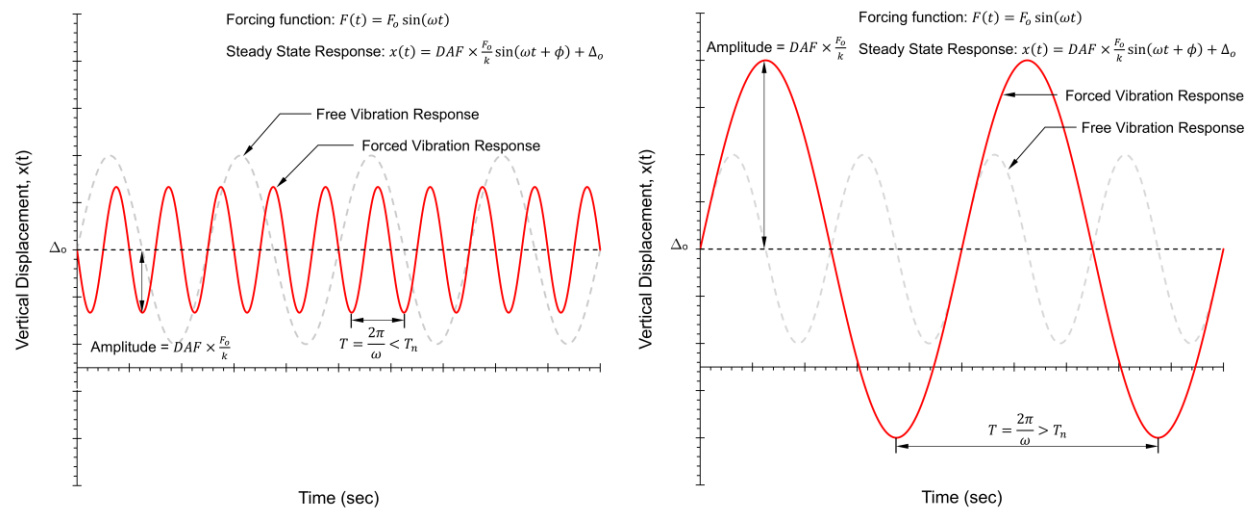


Fig. 19.3 – Forced oscillation for $f/f_n = 2.5$ (left) and $f/f_n = 0.5$ (right). Note the influence of the driving frequency on the amplitude of vibration.

A plot showing the influence of f/f_n on the Dynamic Amplification Factor is shown in Fig. 19.4. The first thing which should be noted is that the highest value of the DAF is when the driving frequency is approximately equal to the natural frequency – this is commonly noted as **resonance**. The second observation is that increasing the amount of damping in the system tends to reduce the amplification, especially the peak value at resonance. Finally, the DAF is equal to 1 when f/f_n is equal to zero, and gradually becomes 0 when the ratio f/f_n becomes large.

Designing for Dynamic Effects

Although calculating the complete response of a structure under dynamic loads is necessary in certain situations, in most cases it is sufficient to only check the if maximum stresses which result do not cause the structure to fail due to buckling or yielding. This can be done by calculating the effective static loading which produces the same effect on the structure as the dynamic loads.

Consider a set of dynamic loads, $\mathbf{w}_{\text{total}}$, which has the following form:

$$\mathbf{w}_{\text{total}} = \mathbf{w}_{\text{stationary}} + \mathbf{w}_0 \sin(\omega t) \quad (19.10)$$

Note: w may be an area loading in kPa, a line load in kN/m, or a collection of joint loads in kN.

In Eq. (19.10), $\mathbf{w}_{\text{stationary}}$ refers to the component of the loading which does not vary in time, like the dead load of the structure and the weight of the people as they stand on the structure. The amplitude of the loading is \mathbf{w}_0 , which considers the impact loading on the bridge due to the crowd of people walking around, and the frequency of the impact loading is ω rad/sec (or $f = \omega/2\pi$ cycles/sec). Sample values of these terms for a single person as they walk are shown in Fig. 19.5.

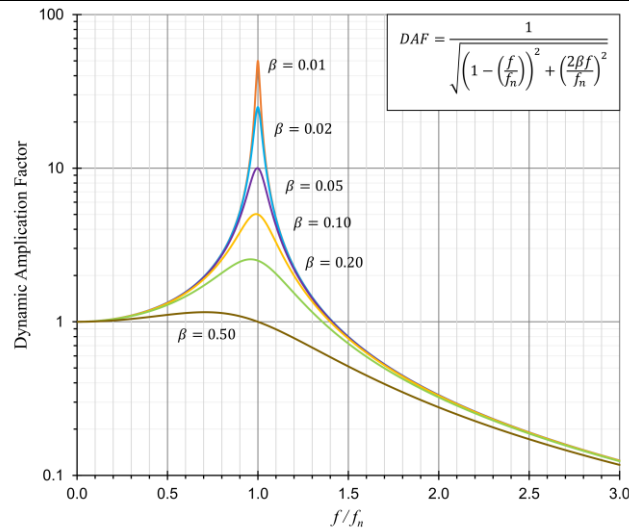


Fig. 19.4 – Influence of f/f_n on the DAF for various values of β

Using Eq. (19.8), the equivalent static load, w_{eq} , is equal to the stationary component of the loading plus an amplified dynamic component. The amplified dynamic component is obtained by taking the amplitude of loading, w_o , and multiplying it by the Dynamic Amplification Factor to consider the interaction between the frequency of loading and the natural frequency, which results in the following:

$$w_{eq} = w_{\text{stationary}} + DAF \times w_o \quad (19.11)$$

Evaluating the DAF is a straightforward process once the damping, β , and the natural frequency of the structure, f_n are known. Two simple equations for calculating the natural frequency for truss or beam structures are shown below in Table 19.1. Once the equivalent static load has been obtained, then the member forces and stresses can be checked.

Table 19.1 – Simple expressions for calculating f_n for truss or beam structures

	Point Load at Midspan	Uniformly Distributed Load
Schematic		
Natural Frequency (Hz)	$f_n = \frac{15.76}{\sqrt{\Delta_o}}$	$f_n = \frac{17.76}{\sqrt{\Delta_o}}$

** Δ_o is the midspan deflection under $w_{\text{stationary}}$ in mm.

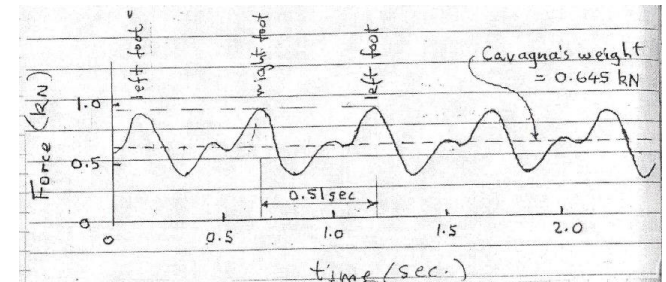


Fig. 19.5 – Time-varying loads caused by a person walking. The stationary component of the load is 0.645 kN with an amplitude of approximately 0.25 kN, occurring at a frequency of approximately 2 Hz.

Note: When designing a pedestrian bridge, the frequency of loading caused by people walking is typically assumed to be 2 Hz. Therefore, unless the bridge contains components which can provide significant amounts of damping, having a natural frequency which is close to 2 Hz will lead to large amounts of amplification and may cause the bridge to collapse.